2011

A Complete Spectroscopic Survey of the Milky Way Satellite Segue 1: The Darkest Galaxy

Joshua D. Simon

Marla Geha

Quinn E. Minor

Beth Willman
Haverford College

The Astrophysical Journal, 733:46 (20pp), 2011 May 20 doi:10.1088/0004-637X/733/1/46

A COMPLETE SPECTROSCOPIC SURVEY OF THE MILKY WAY SATELLITE SEGUE 1: THE DARKEST GALAXY*

Joshua D. Simon[1], Marla Geha[2], Quinn E. Minor[3], Gregory D. Martinez[3], Evan N. Kirby[4,8], James S. Bullock[3], Manoj Kaplinghat[3], Louis E. Strigari[5,8], Beth Willman[6], Philip I. Choi[7], Erik J. Tollerud[3], and Joe Wolf[3]
[1] Observatories of the Carnegie Institution of Washington, 813 Santa Barbara Street, Pasadena, CA 91101, USA; jsimon@obs.carnegiescience.edu
[2] Astronomy Department, Yale University, New Haven, CT 06520, USA; marla.geha@yale.edu
[3] Center for Cosmology, Department of Physics and Astronomy, University of California, Irvine, CA 92697, USA; qminor@uci.edu, gmartine@uci.edu, bullock@uci.edu, mkapling@uci.edu, etolleru@uci.edu, wolfj@uci.edu
[4] California Institute of Technology, Department of Astronomy, MS 249-17, Pasadena, CA 91106, USA; enk@astro.caltech.edu
[5] Kavli Institute for Particle Astrophysics and Cosmology, Stanford University, Stanford, CA 94305, USA; strigari@stanford.edu
[6] Departments of Physics and Astronomy, Haverford College, Haverford, PA 19041, USA; bwillman@haverford.edu
[7] Department of Physics and Astronomy, Pomona College, Claremont, CA 91711, USA; pic04747@pomona.edu
Received 2010 July 26; accepted 2011 March 10; published 2011 May 3

ABSTRACT

We present the results of a comprehensive Keck/DEIMOS spectroscopic survey of the ultra-faint Milky Way satellite galaxy Segue 1. We have obtained velocity measurements for 98.2% of the stars within 67 pc (10′, or 2.3 half-light radii) of the center of Segue 1 that have colors and magnitudes consistent with membership, down to a magnitude limit of $r = 21.7$. Based on photometric, kinematic, and metallicity information, we identify 71 stars as probable Segue 1 members, including some as far out as 87 pc. After correcting for the influence of binary stars using repeated velocity measurements, we determine a velocity dispersion of $3.7^{+1.4}_{-1.1}$ km s^{-1}. The mass within the half-light radius is $5.8^{+8.2}_{-3.1} \times 10^5\ M_\odot$. The stellar kinematics of Segue 1 require very high mass-to-light ratios unless the system is far from dynamical equilibrium, even if the period distribution of unresolved binary stars is skewed toward implausibly short periods. With a total luminosity less than that of a single bright red giant and a V-band mass-to-light ratio of 3400 $M_\odot/L_\odot$, Segue 1 is the darkest galaxy currently known. We critically re-examine recent claims that Segue 1 is a tidally disrupting star cluster and that kinematic samples are contaminated by the Sagittarius stream. The extremely low metallicities ([Fe/H] < -3) of two Segue 1 stars and the large metallicity spread among the members demonstrate conclusively that Segue 1 is a dwarf galaxy, and we find no evidence in favor of tidal effects. We also show that contamination by the Sagittarius stream has been overestimated. Segue 1 has the highest estimated dark matter density of any known galaxy and will therefore be a prime testing ground for dark matter physics and galaxy formation on small scales.

Key words: dark matter – galaxies: dwarf – galaxies: individual (Segue 1) – galaxies: kinematics and dynamics – Local Group

Online-only material: color figures, machine-readable table

1. INTRODUCTION

The Sloan Digital Sky Survey (SDSS) has been tremendously successful in revealing new Milky Way dwarf galaxies over the past five years (e.g., Willman et al. 2005; Zucker et al. 2006; Belokurov et al. 2007a, 2010; Walsh et al. 2007). However, its limited depth and sky coverage, along with the difficulty of obtaining spectroscopic follow-up observations, still leave us with an incomplete understanding of the Milky Way's satellite population. In particular, key parameters such as the luminosity function, mass function, radial distribution, and total number of satellites depend extremely sensitively on the properties of the few least luminous dwarfs (e.g., Tollerud et al. 2008), which are not yet well determined. Since the least luminous dwarfs are the closest and densest known dark matter halos to the Milky Way, these same objects represent critical targets for indirect dark matter detection experiments (e.g., Baltz et al. 2000; Evans et al. 2004; Colafrancesco et al. 2007; Strigari et al. 2008b; Kuhlen et al. 2008; Bringmann et al. 2009; Pieri et al. 2009; Martinez et al. 2009) and for placing limits on the phase-space density of dark matter particles (e.g., Hogan & Dalcanton 2000; Dalcanton & Hogan 2001; Kaplinghat 2005; Simon & Geha 2007; Strigari et al. 2008b; Geha et al. 2009). However, as the closest known satellites to the Milky Way, they are also the most susceptible to tidal forces and other observational systematics.

Because of the extreme lack of bright stars in these systems, most of the faintest dwarfs such as Willman 1 (Willman et al. 2005), Boötes II (Walsh et al. 2007), Segue 1 (Belokurov et al. 2007a), and Segue 2 (Belokurov et al. 2009) remain relatively poorly characterized by observations; for example, the dynamical state of Willman 1 has still has not been established (Martin et al. 2007; Willman et al. 2010), and the velocity dispersion of Boo II is uncertain at the factor of ∼5 level (Koch et al. 2009). Similarly, although Geha et al. (2009, hereafter G09) demonstrated that the kinematics of stars in Segue 1 clearly indicate that it is a dark matter-dominated object, other observations have suggested the possibility of tidal debris in the vicinity of Segue 1, as well as potential contamination from the Sagittarius stream (Niederste-Ostholt et al. 2009).

More generally, the issues of tidal disruption (e.g., Peñarrubia et al. 2008) and binary stars (McConnachie & Côté 2010) are the last remaining major questions to be settled regarding the nature of the faintest dwarfs. These objects promise clues to the

* The data presented herein were obtained at the W. M. Keck Observatory, which is operated as a scientific partnership among the California Institute of Technology, the University of California, and NASA. The Observatory was made possible by the generous financial support of the W. M. Keck Foundation.
[8] Hubble Fellow

extreme limits of galaxy formation (Gilmore et al. 2007; Strigari et al. 2008a) and perhaps to the formation of the first galaxies in the early universe (e.g., Bovill & Ricotti 2009), as well as offering insights into dark matter physics. However, these applications hinge on the assumption that the mass distribution of each system is accurately known. Current mass estimates assume dynamical equilibrium and that the observed kinematics are not being affected by Galactic tides or binary stars, but tests of those assumptions are obviously required in order to confirm that the dwarfs are bound, equilibrium systems. If instead the observed velocity dispersions of Segue 1, Willman 1, and others are being inflated either by the tidal influence of the Milky Way or the presence of binary stars in the kinematic samples, then they are unlikely to be useful probes of the behavior of dark matter on small scales.

Correcting velocity dispersions for binaries, which are inevitably present in any stellar system, is relatively straightforward (Minor et al. 2010). The only observational requirement is that a significant subset of the sample have at least two velocity measurements with a separation of order 1 yr. Tidal effects, unfortunately, are more difficult to nail down. The only unambiguous signature of tidal interactions is the presence of tidal tails (e.g., Toomre & Toomre 1972). Detecting such features in the ultra-faint dwarfs is extremely challenging: the galaxies themselves have central surface brightnesses of 26–28 mag arcsec^{-2} (Martin et al. 2008), so any tidal debris would be at least several magnitudes fainter and likely below the SDSS detection limit of $\sim$30 mag arcsec^{-2}. Deeper, wide-field photometric surveys of the ultra-faint dwarfs can reach surface brightnesses as low as 32.5 mag arcsec^{-2} (Sand et al. 2009, 2010; Muñoz et al. 2010; de Jong et al. 2010), but such observations are not yet available for most of the dwarfs.

In principle, spectroscopic studies can pinpoint the stars associated with an object and probe debris at lower surface densities than is possible photometrically. Spectroscopic surveys also provide the only means of identifying tidal debris that is oriented along the line of sight to an object (Łokas et al. 2008; Klimentowski et al. 2009). However, the currently available spectroscopic samples of less than 25 stars in the faintest dwarfs are not sufficient to determine to what extent tides may be affecting the kinematics. Much larger spectroscopic data sets are required to test for tidal effects.

In this paper, we present a nearly complete spectroscopic survey of Segue 1 that is aimed at obtaining repeated velocity measurements of known members and searching for stars that have been tidally stripped from the system. We describe our modeling of the binary star population and the mass distribution in more detail in a companion paper (Martinez et al. 2010, hereafter Paper II), and a separate study examines the implications of our new mass measurements for indirect detection of dark matter (Essig et al. 2010). In Section 2, we describe the survey and the data reduction. We identify Segue 1 member stars in Section 3 and then analyze their metallicities and velocities in Section 4. In Section 5, we present our derivation of the intrinsic velocity dispersion of Segue 1 after correcting for the presence of binary stars in the sample (see Paper II for more details), and in Section 6 we describe our detection of an unrelated tidal stream in the same part of the sky. We consider the implications of this data set for proposals that the kinematics of Segue 1 are affected by contamination and tidal disruption in Section 7. We discuss the utility of Segue 1 for placing constraints on the properties of dark matter in Section 8. In Section 9, we summarize our findings and conclude.

Table 1
Summary of Properties of Segue 1

Row	Quantity	Value
(1)	R.A. (J2000) (h m s)	$10:07:03.2 \pm 1\overset{s}{.}7$
(2)	Decl. (J2000) ($^\circ$ $'$ $''$)	$+16:04:25 \pm 15''$
(3)	Distance (kpc)	23 ± 2
(4)	M_V	$-1.5^{+0.6}_{-0.8}$
(5)	L_V ($L_\odot$)	340
(6)	ϵ	$0.48^{+0.10}_{-0.13}$
(7)	$\mu_{V,0}$ (mag arcsec^{-2})	$27.6^{+1.0}_{-0.7}$
(8)	$r_{\rm eff}$ (pc)	29^{+8}_{-5}
(9)	$V_{\rm hel}$ (km s^{-1})	208.5 ± 0.9
(10)	$V_{\rm GSR}$ (km s^{-1})	113.5 ± 0.9
(11)	σ (km s^{-1})	$3.7^{+1.4}_{-1.1}$
(12)	Mass ($M_\odot$)	$5.8^{+8.2}_{-3.1} \times 10^5$
(13)	M/L_V ($M_\odot/L_\odot$)	3400
(14)	Mean [Fe/H]	-2.5

Notes. Rows (1)–(2) and (4)–(8) are taken from the SDSS photometric analysis of Martin et al. (2008) and row (3) from Belokurov et al. (2007a). Values in rows (9)–(14) are derived in this paper.

2. EXPERIMENTAL DESIGN, OBSERVATIONS, AND DATA REDUCTION

2.1. A Survey for Tidal Debris

As a complement to ongoing deep, wide-field photometric surveys of the ultra-faint dwarfs (e.g., Muñoz et al. 2010), we embarked upon a spectroscopic search for evidence of tidal stripping or extratidal stars. The ideal target for such a search would be a galaxy that (1) is nearby, to maximize the tidal forces it is currently experiencing,[9] (2) is moving at a high velocity relative to the Milky Way, to minimize the degree of contamination by foreground stars, and (3) has a small angular size, to minimize the area that the survey needs to cover. Out of all the known Milky Way dwarf galaxies, the clear choice according to these criteria is Segue 1. At a distance of 23 kpc from the Sun (28 kpc from the Galactic center), Segue 1 is the closest dwarf galaxy other than Sagittarius, which of course is the prototype for a dwarf undergoing tidal disruption. Its heliocentric velocity of 207 km s^{-1} (the largest of the Milky Way satellites within 200 kpc) and relatively small velocity dispersion give Segue 1 the lowest expected surface density of Milky Way foreground stars within 3σ of its mean velocity (according to the Besançon model; Robin et al. 2003). Finally, if Segue 1 is *not* surrounded by a massive dark matter halo—and it can only host visible tidal features if no extended halo is present—its instantaneous Jacobi (tidal) radius based on the stellar mass estimated by Martin et al. (2008) is $\sim$30 pc, or $4\overset{'}{.}5$, which is an observationally feasible area to search. This calculation conservatively assumes that Segue 1 has never been closer to the Milky Way than it is now; if its orbital pericenter is less than 28 kpc, its baryon-only tidal radius would be even smaller. The properties of Segue 1 are summarized in Table 1.

2.2. Target Selection

To select targets for the survey, we focused on the area within $\sim 15'$ (100 pc) of the center of Segue 1 as determined by Martin

[9] If the object is too close to the pericenter of its orbit, though, then the extent of its tails (if they exist) would be minimized.

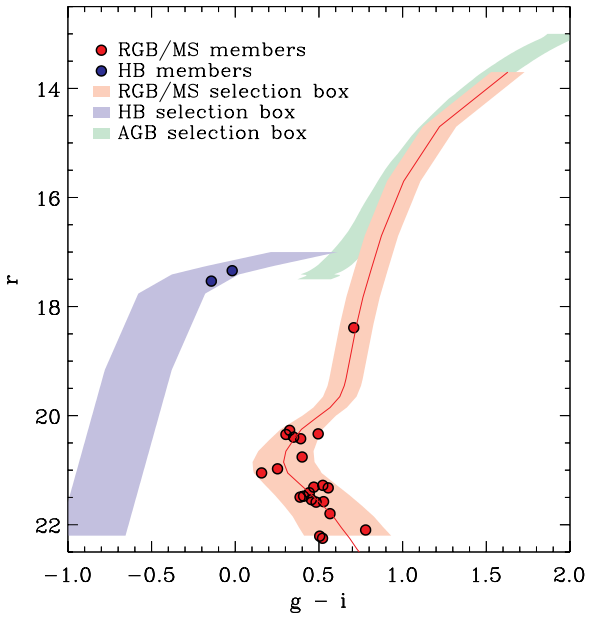

Figure 1. Photometric selection criteria for candidate Segue 1 members. The red giant branch/main-sequence selection region (shaded red) is based on the M92 isochrone of Clem et al. (2008), adjusted slightly at magnitudes fainter than $r = 20.65$ so as to enclose all of the spectroscopically confirmed members from G09 (red line). The blue and green shaded regions represent the horizontal branch (from the M13 isochrone of Clem et al. 2008) and AGB (from a Girardi et al. 2004 theoretical isochrone at [Fe/H] $= -1.7$) selection boxes, respectively. The filled points are the 24 member stars identified by G09.

et al. (2008). Guided by the 24 member stars identified by G09, we tweaked the color of the (appropriately shifted and reddened) M92 isochrone from Clem et al. (2008) so that it passed through the center of the member sequence at all magnitudes (this adjustment was only needed for the subgiant branch and main sequence, not the red giant branch). The Segue 1 main sequence appears to be slightly redder than that of M92, with the offset increasing toward fainter magnitudes (see Figure 1). The full G09 member sample is located within 0.25 mag of the adjusted fiducial track (0.2 mag for $r \leqslant 21$ and 0.1 mag for $r \leqslant 20$).

Using positions and magnitudes extracted from DR5 of the SDSS (Adelman-McCarthy et al. 2007), we selected stars within a narrow range of colors around the adopted fiducial sequence. Red giants ($r \leqslant 20$) were required to be within 0.1 mag of the sequence, and the selection window was gradually widened toward fainter magnitudes, reaching 0.235 mag at $r = 21.7$. Horizontal branch (HB) candidates were allowed to be 0.2 mag away from the fiducial track. A small number of stars located near a metal-poor asymptotic giant branch (AGB) isochrone from Girardi et al. (2004) were also selected. Within 10′ (67 pc) of Segue 1, we identified 112 stars lying within the color–magnitude selection box (down to a magnitude limit of $r = 21.7$) that we consider to be our primary target sample. Stars up to a factor of two farther away from the fiducial sequences or within the primary color–magnitude selection region but at larger distances from Segue 1 were targeted with reduced priorities. We also included as many of the known member stars as possible on multiple slit masks to obtain repeated velocity measurements for constraining the binary population.

2.3. Observations

We observed 12 new slit masks, including at least one slit placed on each of the 112 candidate member stars (plus repeat observations of 18 of the 24 members from G09), with the DEIMOS spectrograph (Faber et al. 2003) on the Keck II telescope. The observations took place on the nights of 2009 February 18, 26, and 27 and 2010 February 12 and 13.

The spectrograph setup and observing procedures were identical to those described by Simon & Geha (2007, hereafter SG07): we used the 1200 ℓ mm^{-1} grating with an OG550 filter to cover the wavelength range 6500–9000 Å at a spectral resolution of $R = 6000$ (slit width of 0.″7). An internal quartz lamp and Kr, Ar, Ne, and Xe arc lamps were employed for flat-fielding and wavelength calibration, respectively. Total integration times for the science masks ranged from 10 minutes for a mask targeting very bright stars to ∼2 hr for most of the masks aimed at fainter stars. The masks are summarized in Table 2. Conditions during the observing nights were generally good, with seeing ranging from 0.″7 to 1.″0 and thin cirrus at times.

2.4. Data Reduction

As with the observations, data reduction followed the outline given in SG07. We used a modified version of the data reduction pipeline developed for the DEEP2 galaxy redshift survey. The additional improvements we made to the code since SG07 were to redetermine the wavelength solution for slits that were initially not fit well and to identify and extract serendipitously observed sources more robustly. The pipeline determines a wavelength solution for each slit, flat-fields the data, models and subtracts the sky emission, removes cosmic rays, co-adds the individual frames, and then extracts the spectra.

In the spring of 2009, the DEIMOS CCD array was experiencing an intermittent problem wherein one of the eight chips (corresponding to the blue half of the spectral range at one end of the field of view) would fail to read out completely on some exposures. In a few cases, the affected chip was completely blank, while in others only the top or bottom of the chip was absent and the remainder of the pixels were saved normally. We dealt with this problem conservatively by excluding all of the data from the temperamental chip from our reduction any time it exhibited abnormal behavior. As a result, a fraction of our targets have lower signal-to-noise ratio (S/N) in the blue than would be expected from the total mask observing times, but since most of the key spectral features for our analysis are on the red side of the spectra, the overall impact is minor.

After reducing the data, we used the custom IDL code described by SG07 to measure the radial velocity of each star. We first corrected each spectrum for velocity offsets that could result from miscentering of the star in the slit by cross-correlating the telluric absorption features against those of a telluric standard star specially obtained for this purpose (Sohn et al. 2007; SG07). The spectra were then cross-correlated with a library of high S/N templates with well-known velocities obtained with DEIMOS in 2006 and 2007. The template library contains 15 stars ranging from spectral type F through M, mostly focusing on low-metallicity giants but also including representative examples of subgiants, HB stars, main-sequence stars, and more metal-rich giants. We also fit four extragalactic templates, identifying a total of 69 background galaxies and quasars. The velocity of each target spectrum is determined from the cross-correlation with the best-fitting template spectrum. We estimate velocity errors using the Monte Carlo technique presented in SG07: we add random noise to each spectrum 1000 times and then redetermine its velocity in each iteration. We take the standard deviation of the Monte Carlo velocity distribution for each star as its measurement uncertainty. Previous analysis of a

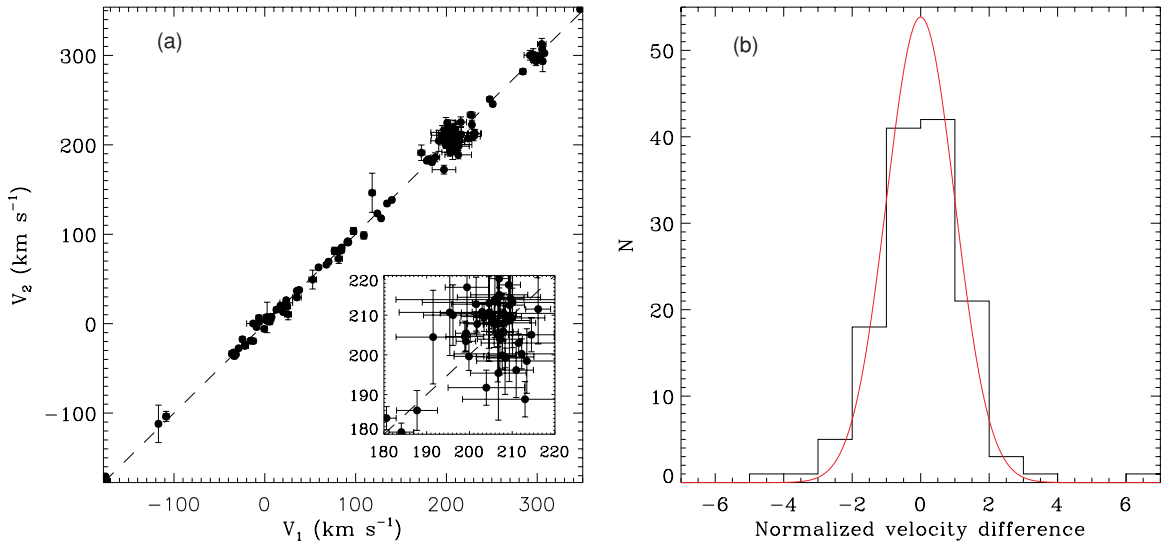

Figure 2. (a) Comparison of velocity measurements for the sample of stars observed at least twice. The inset shows a zoomed-in view of the velocity range near Segue 1. (b) Histogram of velocity differences between repeat observations, normalized by their uncertainties ($(v_2 - v_1)/\sqrt{\sigma_1^2 + \sigma_2^2}$). The red curve is a Gaussian with unit dispersion, which the data should follow if the measurement uncertainties are correct. The larger than expected number of stars in the wings of the distribution is caused by the presence of binaries and RR Lyrae variables in the sample.

(A color version of this figure is available in the online journal.)

Table 2
Keck/DEIMOS Slit Masks

Mask Name	α (J2000) (h m s)	δ (J2000) (° ′ ″)	P.A. (deg)	t_{exp} (s)	MJD of Observation	No. of Slits	% Useful Spectra
Segue1-1[a]	10 07 06.01	16 02 56.1	65.0	5400	54416.551	59	88%
Segue1-2	10 07 08.85	16 04 51.9	180.0	7200	54881.311	65	83%
Segue1-3	10 07 00.82	16 06 59.6	−57.0	5400	54881.416	61	92%
Segue1-C	10 06 39.29	16 06 02.0	171.0	600	54881.284	38	87%
Segtide1	10 06 57.65	16 10 20.5	178.0	7500	54889.267	48	88%
Segtide2	10 06 36.07	16 07 39.6	171.0	7500	54889.343	48	90%
Segtide3	10 07 34.37	16 10 28.9	144.0	7500	54889.444	47	94%
Segtide4	10 06 19.07	16 01 34.7	179.0	7350	54890.243	50	84%
Segtide5	10 07 40.78	15 56 22.1	1.0	7800	54890.342	44	89%
Segtide6	10 06 59.81	15 56 50.8	−78.0	7200	54890.444	54	93%
Segtide7	10 07 14.20	15 55 43.9	−123.0	2700	54889.542	49	76%
Segtide8	10 06 58.45	16 03 37.4	−134.0	1200	55240.355	40	90%
Segtide9	10 07 07.83	15 56 24.7	−165.0	1800	55240.402	48	85%

Note. [a] Segue1-1 is the slit mask observed by G09. For consistency, we use the velocities reported in that paper rather than re-reducing the mask and measuring the velocities again.

sample of stars observed multiple times with the same instrument configuration and analysis software indicates that our velocity accuracy is limited by systematics at the 2.2 km s^{-1} level. We have now confirmed the magnitude of the systematic errors with a much larger sample of repeat measurements than were used by SG07.

2.5. Repeat Measurements

As discussed in Sections 1 and 2.2, one of the main goals of this study is to determine the effect of binary stars on the observed velocity dispersion of Segue 1. Accomplishing this task requires making multiple velocity measurements of stars, verifying that the derived velocity uncertainties are accurate, and searching for individual binaries. The bulk of our analysis of the repeat observations is presented in Paper II, but in Figure 2(a) we illustrate the agreement between subsequent velocity measurements and the initial one for each star observed more than once. Figure 2(b) shows the distribution of velocity differences for each pair of measurements, normalized by their uncertainties. The good match to a Gaussian distribution for $-2 < (v_2 - v_1)/\sqrt{\sigma_1^2 + \sigma_2^2} < 2$ indicates that the uncertainties are accurate, and the excess in the wings of the distribution provides evidence for velocity variability (see Section 4.2 and Paper II). A total of 93 stars, including approximately half of the member sample, were observed at least twice during the course of our survey.

2.6. Spectroscopic Completeness

In Section 2.3, we described obtaining a spectrum of each one of the 112 stars within our primary photometric selection region and not more than 67 pc from the center of Segue 1. We successfully measured velocities for 109 of these stars. One target star (SDSSJ100707.12+160022.4) did not have any identifiable features in its spectrum, one spectrum (SDSSJ100700.75+160300.5) suffered from reduction difficulties (see the Appendix), although it appears to be a member,

Table 3
Segue 1 Velocity Measurements

Star	Velocity (km s^{-1})	ΣCa (Å)	Radius (arcmin)	MJD	g	r	i	Member (Subjective)[a]	EM Member Prob.[b]	Bayesian Member Prob.[c]
SDSSJ100613.98+155436.1	-46.8 ± 4.6	3.3 ± 0.6	15.4	54890.243	24.28	22.64	21.17	0	−9.999	−9.999
SDSSJ100614.24+160424.7	-66.7 ± 2.4	2.4 ± 0.3	11.8	54890.243	20.29	19.97	19.81	0	0.000	0.000
SDSSJ100614.31+160050.9	150.1 ± 3.3	2.9 ± 0.5	12.3	54890.243	21.52	21.03	21.13	0	0.000	0.000
SDSSJ100614.40+160013.0	70.1 ± 2.2	4.8 ± 0.3	12.5	54890.243	17.14	16.44	16.16	0	0.000	0.000
SDSSJ100614.78+155512.7	45.2 ± 2.9	1.5 ± 0.4	14.8	54890.243	24.83	22.50	21.06	0	−9.999	−9.999
SDSSJ100614.87+160858.7	29.1 ± 2.9	4.4 ± 0.4	12.5	54890.243	20.09	19.55	19.32	0	0.000	0.000
SDSSJ100615.16+155556.6	54.3 ± 2.6	2.9 ± 0.3	14.3	54890.243	22.30	21.07	19.96	0	−9.999	−9.999
SDSSJ100615.53+160056.9	-6.7 ± 2.7	1.7 ± 0.4	12.0	54890.243	21.04	20.73	20.65	0	0.000	0.000
SDSSJ100616.95+160524.3	-10.0 ± 2.4	3.3 ± 0.3	11.2	54890.243	23.22	21.47	20.39	0	−9.999	−9.999
SDSSJ100617.35+155606.6	1.7 ± 2.4	2.1 ± 0.4	13.8	54890.243	22.81	21.47	20.68	0	−9.999	−9.999

Notes.
[a] Member status according to the criteria established at the beginning of Section 3.1. 1 indicates membership, and 0 is for non-members.
[b] Membership probability from the EM algorithm. The algorithm is run on the subset of stars whose colors and magnitudes are consistent with membership, so photometric non-members are indicated by probability −9.999.
[c] Membership probability from the Bayesian approach. As with the EM algorithm, these calculations are run on the subset of stars whose colors and magnitudes are consistent with membership, so photometric non-members are indicated by probability −9.999.
(This table is available in its entirety in a machine-readable form in the online journal. A portion is shown here for guidance regarding its form and content.)

and the remaining one (SDSSJ100733.12+155736.7) was not detected in our data. The magnitude of this latter star should have made it easily visible in the exposures we obtained, but a check of the SDSS images showed no source at this position, and the target was flagged in the SDSS catalog as a possible moving object. We conclude that this source was actually an asteroid that happened to have the right colors and position to be selected for our survey. After excluding it, our completeness is 98.2%. We also targeted a fraction of Segue 1 member candidates as far out as 16′ (107 pc). Within 11′, 12′, and 13′, our overall completeness is 97.0%, 96.7%, and 92.3%, respectively. Only a few stars at larger radii were observed.

3. DEFINING THE SEGUE 1 MEMBER SAMPLE

In total (including the observations of G09), we obtained 528 good spectra of 394 individual stars, of which 162 were classified as high-priority member candidates (109 within 10′ of the center of Segue 1 and 58 at larger radii) according to the criteria described in Section 2.2. We present all of our velocity and Ca triplet (CaT) equivalent width (EW) measurements in Table 3. Our repeat velocity measurements for 93 of these stars span a maximum time baseline of 2.25 years. We use a variety of techniques to identify Segue 1 member stars in this data set. The primary data available for distinguishing members from non-members are color/magnitude, velocity, metallicity (either in the form of [Fe/H] estimated from the CaT lines or simply the raw CaT EW), spatial position, and the strength of the Na I λ8190 doublet.[10]

3.1. Methods of Identifying Segue 1 Members

We consider three different membership selection techniques: a subjective, star-by-star selection using velocity, metallicity, color, magnitude, and the spectrum itself, a slightly modified version of the algorithm introduced by Walker et al. (2009b), and a new Bayesian approach presented in Paper II. For the remainder of the paper, we adopt the third method as defining our primary sample except where explicitly noted.

We first select member stars using the parameters listed above. Candidate members must have colors and magnitudes consistent with the photometric selection region displayed in Figure 1 and described in Section 2.2, must have velocities within a generous $\sim 4\sigma$ window around Segue 1 based on the systemic velocity and velocity dispersion measured by G09, and should have low metallicities. We can then iteratively refine the member selection by examining the stars near the boundaries of the selection region more carefully. With this process, we classify 65 stars as definite members, six additional stars as probable members, and five more as likely (but not certain) non-members. The remaining stars are clearly not members. The sample selected in this way is displayed in Figure 3.

While the flexibility afforded by this subjective approach is useful and allows all available information to be taken into account, a rigorous and objective method is also desirable to avoid the possibility of bias. Walker et al. (2009b) recently developed such a statistical algorithm to separate two potentially overlapping populations. This technique, known as expectation maximization (EM), allows one to estimate the parameters of a distribution in the presence of contamination, with specific application to the case of identifying dwarf galaxy member stars against a Milky Way foreground. Given a set of velocities, radial distances, and a third parameter in which dwarf galaxy stars and Milky Way stars are distributed differently, the EM algorithm relies on the distinct distributions of the two populations in each property to iteratively assign membership probabilities to each star until it converges on a solution. Walker et al. (2009b) use the pseudo-EW of the Mg triplet lines at 5180 Å as their third parameter, but we find that the reduced EW of the CaT lines works as well. Rutledge et al. (1997a, 1997b) define this reduced EW as $W' = \Sigma\mathrm{Ca} - 0.64(V_{\mathrm{HB}} - V)$, where ΣCa is the weighted sum of the EWs of the CaT lines: $\Sigma\mathrm{Ca} = 0.5\mathrm{EW}_{8498} + 1.0\mathrm{EW}_{8542} + 0.6\mathrm{EW}_{8662}$. Note that since the EM algorithm does not incorporate photometric information, it must be run on a sample of stars that has already passed the color–magnitude selection. Also, EM may fail to select HB stars because their

[10] We note, however, that the Na lines only function as a way to distinguish dwarfs from giants for very red stars ($V - I \gtrsim 2$), significantly redder than anything we expect to find in a low-luminosity, low-metallicity system like Segue 1 (Gilbert et al. 2006). Also, because of the tiny number of giants in Segue 1, the majority of the *member* stars are actually on the main sequence rather than the giant branch. Therefore, the strength of the Na doublet primarily serves to eliminate stars that were already obvious non-members from consideration.

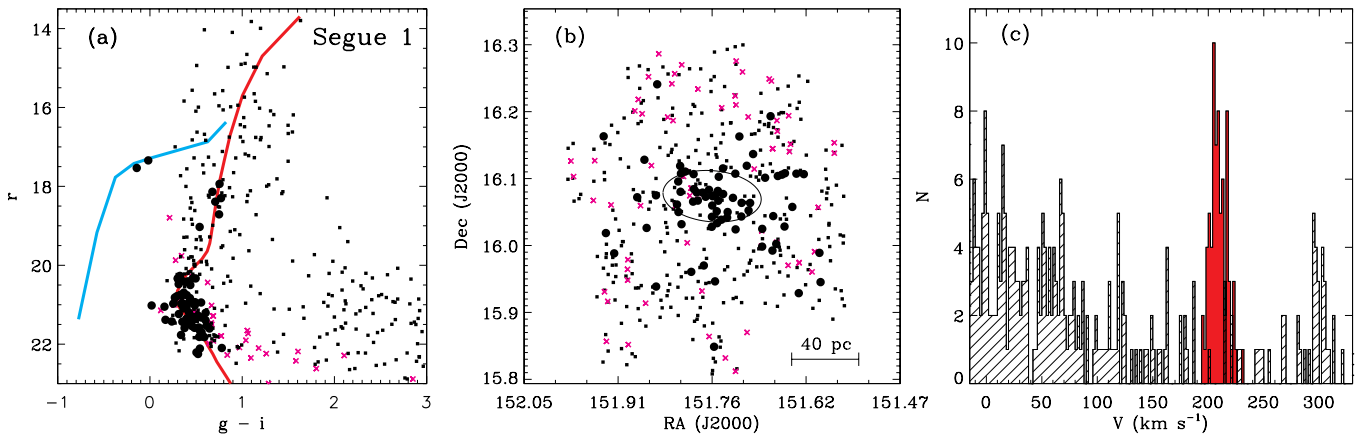

Figure 3. (a) Color–magnitude diagram of observed stars in Segue 1. The large black circles represent the 71 stars identified as definite or probable radial velocity members of the galaxy using our subjective approach, the small black dots represent stars identified as likely or certain non-members, and the magenta crosses are spectroscopically confirmed background galaxies and quasars. The red curve shows the location of the red giant branch, subgiant branch, and main-sequence turnoff populations in the globular cluster M92 and the cyan curve shows the location of the horizontal branch of M13, both corrected for Galactic extinction and shifted to a distance of 23 kpc (data from Clem et al. 2008). (b) Spatial distribution of observed stars in Segue 1. Symbols are the same as in (a), and the ellipse represents the half-light radius of Segue 1 from Martin et al. (2008). (c) Velocity histogram of observed stars in Segue 1. Velocities are corrected to the heliocentric rest frame. The filled red histogram represents stars classified as members, and the hatched black-and-white histogram represents non-members. The velocity bins are 2 km s^{-1} wide.

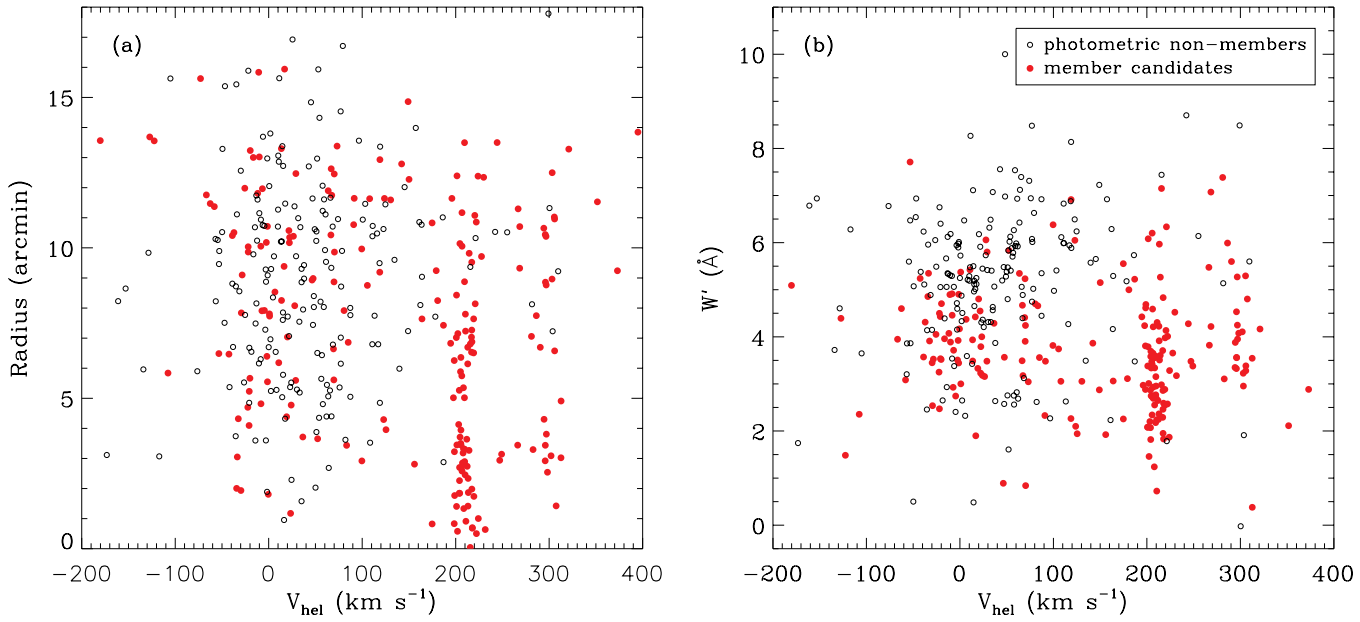

Figure 4. (a) Distribution of observed stars in velocity and radius. Filled red points represent stars that pass the color and magnitude selection (at either high or low priority) described in Section 2.2, and open black points are stars that lie outside that selection region. Stars that have been observed multiple times are plotted with their weighted average values. Segue 1 stands out as the large overdensity of stars near $v_{hel} = 200$ km s^{-1} extending out to a radius of $\sim 13'$. Based on the distribution of Milky Way stars, it is clear that at small radii ($r \leqslant 7'$) the level of contamination of the Segue 1 member sample is very low. In addition to Segue 1, there is also a distinct concentration of stars near 300 km s^{-1}. (b) Distribution of observed stars in velocity and reduced CaT EW, a proxy for metallicity. As in the left panel, a large fraction of the Segue 1 members separate cleanly from the Milky Way foreground population. At $W' > 5$ Å, the distributions begin to overlap, and unambiguously classifying individual stars as members or non-members becomes more difficult. Fortunately, relatively few stars are located in this region. It is clear that Segue 1 is more metal-poor than the bulk of the foreground population, although W' is a much less accurate metallicity indicator for main-sequence stars than giants. The 300 km s^{-1} structure appears to be more enriched than Segue 1.

broad hydrogen lines interfere with measurements of the CaT EW; fortunately, the HB members of Segue 1 are obvious.

We display the distribution of observed stars in radius, velocity, and reduced CaT EW in Figures 4 and 5. Segue 1 stands out as the large overdensity of stars with velocities just above 200 km s^{-1} and smaller than average radii and W' values. We caution that W' is only a properly calibrated metallicity indicator for stars on the red giant branch (RGB), which constitute a small minority of the data set examined here. Nevertheless, experiments with globular cluster stars reaching several magnitudes below the main-sequence turnoff from the compilation of Kirby et al. (2010) show that while W' does increase at constant metallicity toward fainter main-sequence magnitudes, this increase is less than 2 Å for stars within 2 mag of the turnoff. We therefore conclude that including both RGB and main-sequence stars may broaden the Segue 1 distribution toward higher values of W' (perhaps accounting for the clear presence of Segue 1 stars in Figure 4(b) up to $W' \approx 6$ Å), but should not significantly affect the performance of EM.

The EM algorithm selects 68 stars as definite members of Segue 1 (membership probability $p \geqslant 0.9$). An additional three stars have $0.8 \leqslant p < 0.9$ and are classified as members by

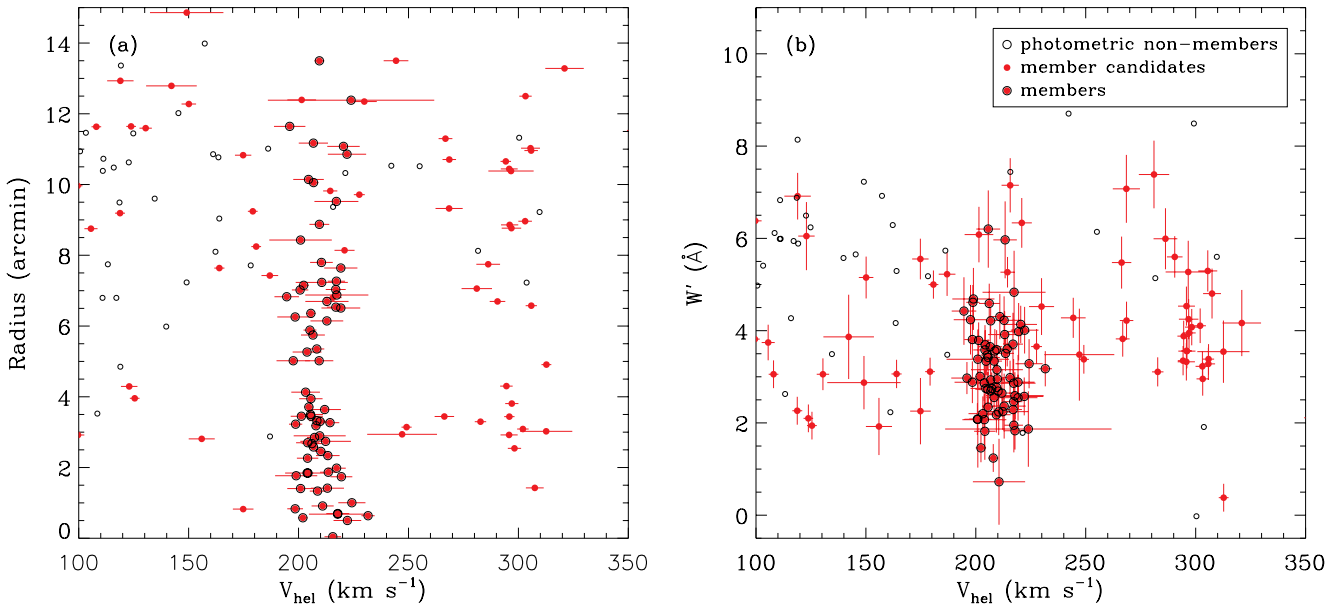

Figure 5. (a) Distribution of observed stars in velocity and radius, zoomed in on Segue 1 and the 300 km s^{-1} stream. Symbols are as in Figure 4, but we have added error bars in velocity and highlighted the subjective 71 star Segue 1 member sample (filled red circles outlined in black). (b) Distribution of observed stars in velocity and reduced CaT EW, zoomed in on Segue 1 and the 300 km s^{-1} stream.

eye, yielding 71 very likely members. These 71 stars correspond to 70 of the 71 subjectively classified members.[11] Finally, three stars have membership probabilities of $0.5 \leqslant p < 0.8$.

Our final results are based on a Bayesian analysis that allows for both contamination by Milky Way foreground stars and the contribution of binary orbital motions to the measured velocities. These calculations are a natural generalization of the Walker et al. (2009b) EM method. The method is described in more detail in Paper II and is summarized here in Section 5. In this framework, we find 53 definite members ($\langle p \rangle \geqslant 0.9$) and nine further probable members ($0.8 \leqslant \langle p \rangle < 0.9$), plus the two RR Lyrae variables (see Section 4.2), but seven of the stars considered likely members by the other two techniques receive lower probabilities of $0.4 \leqslant \langle p \rangle < 0.8$ here. With the exception of the discussion in Section 4.3, where we mention the range of velocity dispersions that can be obtained for different member samples, the main results of this paper (including the velocity dispersion, mass, and density of Segue 1) rely on this Bayesian analysis. It is important to note that unlike previous studies, *we include all stars that pass our photometric cuts in the Bayesian calculations, not just the ones with high membership probabilities*. Each star is weighted according to its probability of being a member of Segue 1. This approach allows us to account correctly for the significant number of stars with membership probabilities that are neither close to zero nor close to one.

4. METALLICITY AND KINEMATICS OF SEGUE 1

4.1. Stellar Metallicities and the Nature of Segue 1

One of the defining differences between galaxies and globular clusters is that dwarf galaxies universally exhibit signs of internal chemical evolution and contain stars with a range of metallicities, while globulars generally do not. Recent work has shown that multiple stellar populations with different chemical abundance patterns are in fact present in some globular clusters, but these differences tend to be subtle (which is why they are only being recognized now) and are preferentially found in luminous clusters that are often argued to be the remnants of tidally stripped dwarf galaxies (e.g., Lee et al. 1999; Marino et al. 2009; Da Costa et al. 2009; Ferraro et al. 2009; Cohen et al. 2010).

We use the spectral synthesis method introduced by Kirby et al. (2008a) and refined by Kirby et al. (2009, 2010) to measure iron abundances[12] in Segue 1 directly from our medium-resolution spectra. Kirby et al. (2010) showed that the metallicities measured in this way are reliable for stars with $\log g < 3.6$. Thus, we can only determine metallicities for the six red giant members of Segue 1; the fainter stars are all at or below the main-sequence turnoff. The metallicities of these six stars span an enormous range, with two stars at [Fe/H] > -1.8 and two others at [Fe/H] < -3.3 (see Table 4). One of the two extremely metal-poor (EMP) stars does not have a well-defined metallicity measurement because no Fe lines are detected in its spectrum. The upper limit on its metallicity therefore depends on the assumptions, but it is certainly well below [Fe/H] $= -3$. The mean metallicity of the Segue 1 red giants is [Fe/H] $= -2.5$, comparable to the most metal-poor galaxies identified so far (Kirby et al. 2008b), and the standard deviation, while not well constrained with such a small sample, is ∼0.8 dex. Using a completely independent data set, Norris et al. (2010b) reach essentially identical conclusions regarding the Segue 1 abundance range and identify yet another EMP member star at [Fe/H] $= -3.5$ (Norris et al. 2010a).

The very large star-to-star spread in metallicities and the presence of EMP stars with [Fe/H] < -3.0 each independently

[11] The EM algorithm includes one star (SDSSJ100711.80+160630.4) with a velocity of 247.1 ± 15.9 km s^{-1} that we rated as too far removed from the systemic velocity to be a member candidate and gives one star (SDSSJ100622.85+155643.0) with a closer velocity but an even larger uncertainty ($v_{hel} = 223.9 \pm 37.8$ km s^{-1}) a lower membership probability of $p = 0.73$. Both of these stars are discussed further in the Appendix.

[12] For historical reasons, these calculations use a solar iron abundance of $12 + \log \epsilon(\mathrm{Fe}) = 7.52$ (Anders & Grevesse 1989), but the difference between this assumption and the modern value of $12 + \log \epsilon(\mathrm{Fe}) = 7.50 \pm 0.04$ (Asplund et al. 2009) is negligible.

Table 4
Segue 1 Metallicity Measurements

Star	g	r	i	$T_{\rm eff}$	log g	[Fe/H]	Number of Measurements	Dispersion Between Measurements
SDSSJ100702.46+155055.3	18.48	17.94	17.73	5148 ± 102	2.64	-2.48 ± 0.15	2	0.42 dex
SDSSJ100714.58+160154.5	18.83	18.30	18.06	5102 ± 109	2.78	-1.73 ± 0.14	3	0.07 dex
SDSSJ100652.33+160235.8	18.87	18.39	18.16	5271 ± 132	2.85	-3.40 ± 0.17	3	0.32 dex
SDSSJ100742.72+160106.9	19.72	18.59	18.14	5251 ± 111	2.76	-2.50 ± 0.14	1	
SDSSJ100710.08+160623.9	19.20	18.71	18.45	5106 ± 109	2.96	-1.63 ± 0.14	4	0.03 dex
SDSSJ100639.33+160008.9	19.44	19.03	18.90	5643 ± 186	3.21	<-3.4	3	

argue that Segue 1 cannot be a globular cluster, contrary to initial suggestions (Belokurov et al. 2007a; Niederste-Ostholt et al. 2009). Only ω Centauri among globular clusters has a comparable metallicity spread (e.g., Norris & Da Costa 1995; Hilker et al. 2004), and that object is widely regarded to be the remnant of a dwarf galaxy (Lee et al. 1999; Majewski et al. 2000b; Carraro & Lia 2000; Hilker & Richtler 2000; Tsuchiya et al. 2003; Mizutani et al. 2003; Rey et al. 2004; Ideta & Makino 2004; McWilliam & Smecker-Hane 2005; Carretta et al. 2010) rather than a true globular. The lowest metallicity Segue 1 giants are also at least a factor of four more metal-poor than any known star in a globular cluster (e.g., King et al. 1998; Kraft & Ivans 2003; Preston et al. 2006; Carretta et al. 2009). We conclude that the metallicities of stars in Segue 1 provide compelling evidence that, irrespective of its current dynamical state, Segue 1 was once a dwarf galaxy.

4.2. Binary and Variable Stars

Before attempting to determine the velocity dispersion and mass of Segue 1, we consider the impact of variable stars and binaries that could be in our sample. The G09 members include two HB stars in Segue 1. Our repeated measurements demonstrate that the velocities of both of these stars vary with time, leading us to conclude that they are RR Lyrae variables. Follow-up photometry with the Pomona College 1 m telescope at Table Mountain Observatory confirms that one of these stars, SDSSJ100644.58+155953.9, is a photometric variable with a characteristic RR Lyrae period of 0.50 days.[13] We do not detect variability in the second star, SDSSJ100705.60+160422.0, but the limits we can place are not inconsistent with the low amplitude variability that might be expected for such a blue star. Given their blue colors, the stars are probably type c variables pulsating in the first overtone mode. Because the light curve phases at the times our spectra were acquired are not known, we cannot measure the center-of-mass velocities of these stars and must remove them from our kinematic sample even though they are certainly members of Segue 1.

We also obtained multiple measurements of five of the six Segue 1 red giants in order to check whether any of them are in binary systems. For four of the stars, the velocity measurements do not deviate by more than 2σ from each other, providing no significant indication of binarity, although long period or low amplitude orbits cannot be ruled out. SDSSJ100652.33+160235.8, however, shows clear radial velocity variability, with the velocity decreasing from 216.1 ± 2.9 km s^{-1} on 2007 November 12 to 203.0 ± 2.3 km s^{-1} on 2009 February 27, and then rising back to 210.8 ± 2.3 km s^{-1} on 2010 February 13. Assuming that these observations correspond to a single orbital cycle, we infer a period of $\sim$1 yr and a companion mass of $\sim 0.65 + 0.25(1/\sin^3 i - 1)\, M_\odot$.

With at least one out of the brightest six stars (excluding the even more evolved HB stars) in the galaxy in a binary system, the binary fraction of Segue 1 is likely to be significant, as has been found for other dwarf galaxies (Queloz et al. 1995; Olszewski et al. 1996) and some, although not all, globular clusters (Fischer et al. 1993; Yan & Cohen 1996; Rubenstein & Bailyn 1997; Clark et al. 2004; Sollima et al. 2007). For main-sequence stars, which dominate our sample, the binary fraction can only be larger since the tight binary systems will not yet have been destroyed by the evolution of the more massive component. We have a limited sample of repeat observations of some of the main-sequence members, in which two additional stars, SDSSJ100716.26+160340.3 and SDSSJ100703.15+160335.0, are detected as probable binaries. However, these binary determinations are almost certainly quite incomplete, and proper corrections for the inflation of the observed velocity dispersion of Segue 1 by binaries must be done in a statistical sense, as we discuss in Section 5.

4.3. Kinematics

Because the issues of membership and binary stars are so critical to our results, we must experiment with different samples of member stars and methods of determining the velocity dispersion. Inspection of Figure 4 makes clear that for $W' \leqslant 3$ Å, the expected contamination by Milky Way foreground stars is negligible (1–2 stars). Very conservatively, then, we can select the stars with $W' \leqslant 3$ Å and 190 km s$^{-1} \lesssim v \lesssim 225$ km s^{-1} as an essentially clean member sample (the exact velocity limits chosen do not matter, since the next closest stars are at $v = 175$ km s^{-1} and $v > 300$ km s^{-1}). With the two RR Lyrae variables and the one obvious RGB binary removed, the velocity dispersion of the other 34 stars is 3.3 ± 1.2 km s^{-1}. (Note that we calculate the velocity dispersion using a maximum likelihood method following Walker et al. 2006.) This value can be regarded in some sense as a lower limit to the observed dispersion of Segue 1 (prior to any correction for undetected binaries).

Since this conservative approach involves discarding nearly half of the data, we would also like to consider alternatives. The largest member sample that we can define is the 71 stars selected using either our holistic, subjective criteria in Section 3.1 or the EM algorithm. After again excluding the two RR Lyraes and the RGB binary, the raw velocity dispersion of these stars is 5.5 ± 0.8 km s^{-1}, which we take as an *upper* limit to the observed dispersion of Segue 1 (as before, prior to correcting for undetected binaries). However, the dispersion in this case is dominated by a single star (SDSSJ100704.35+160459.4; see Section 4.4). If we remove this object from the sample, the

[13] Periods of 0.5 days are of course subject to the possibility of aliasing, and the light curve is not complete enough to rule out a period of 1.0 day. However, such long periods are extremely rare for RR Lyraes, so we consider the 0.50 day period to be the most likely solution.

dispersion of the remaining stars falls to 3.9 ± 0.8 km s^{-1}, corresponding to a factor of two decrease in the mass of the galaxy. Other stars that are borderline members or non-members have negligible effects on the derived dispersion (see the Appendix).

We note at this point a curious finding regarding the brightest stars in Segue 1. If we isolate the evolved stars (six giants and two HB stars) in the sample, their velocity dispersion *appears* to be quite small. For the HB stars and the binary on the giant branch, we cannot assume that we have enough measurements to average out the effects of the binary orbit and RR Lyrae pulsations, but we estimate a dispersion of $1.3^{+2.4}_{-0.7}$ km s^{-1} for the other five RGB stars. Using our full Bayesian analysis (Section 5) and including the binary, the intrinsic dispersion of the giants is $2.0^{+3.1}_{-1.7}$ km s^{-1}. Given the substantial error bars, these values are formally consistent with the larger dispersion obtained for the full data set, even though they are also close to zero. Nevertheless, the velocity dispersion we determine for the remaining stars is not significantly affected by the inclusion or exclusion of the giants and HB stars. Without any known physical mechanism that could change the kinematics of Segue 1 for stars in different evolutionary states, we conclude that the apparently small dispersion of these stars is most likely a coincidence resulting from small number statistics.

Next, we use the sample defined by the Walker et al. (2009b) EM algorithm. Since this sample is nearly identical to that considered in the previous paragraphs, the results are unchanged: a dispersion of 5.7 ± 0.8 km s^{-1} for all 71 stars minus the RR Lyraes and the RGB binary, and 4.1 ± 0.9 km s^{-1} when SDSSJ100704.35+160459.4 is removed. It is worth noting that all of these measurements and those described above are consistent within 1σ with the original velocity dispersion of 4.3 ± 1.2 km s^{-1} determined by G09.

The above two methods make various assumptions about how membership is defined, but do not allow for a fully self-consistent statistical treatment. The method described in Paper II (Martinez et al. 2010) and summarized in Section 5 treats these assumptions and the data analysis in a fully Bayesian manner. This analysis identifies a total of 61 stars (excluding the two RR Lyrae variables) as likely members with $\langle p \rangle > 0.8$. This method arrives at significantly lower membership probabilities for eight stars compared to the EM and subjective analyses. These stars fall into three partially overlapping categories: velocity outliers, frequently with large velocity uncertainties as well (such that there is a significant chance that the star's true velocity is far away from the systemic velocity of Segue 1); stars with large reduced CaT EWs ($W' > 4$ Å); and stars at large radii ($r > 10'$). The only one of these stars that has an appreciable effect on the velocity dispersion is SDSSJ100704.35+160459.4. Removing each of the seven other stars from the sample changes the dispersion by less than 0.2 km s^{-1}. With only the 61 most likely members included in the calculation, we find a velocity dispersion of 3.4 ± 0.9 km s^{-1}.

4.4. Individual Stars With Ambiguous Membership

Despite our best efforts to define a member sample that is both clean and complete, there are fundamental uncertainties that cannot be avoided in determining whether any given star is a member of Segue 1. In particular, we know that Segue 1 is an old, metal-poor stellar system located 23 kpc from the Sun, and moving at a heliocentric velocity of $\sim$207 km s^{-1}. Unfortunately, the Milky Way halo also contains old, metal-poor stars that span ranges in distance and velocity that encompass Segue 1. Given a large enough search volume, it is therefore inevitable that some halo stars with the same age, metallicity, distance (and hence the same colors and magnitudes), and velocity as Segue 1 will be found. We can use observations and models to estimate the *expected number* of such stars included in our survey, but that does not help us in ascertaining the provenance of individual stars.

As a result, we are left with a small number of stars whose membership status is necessarily uncertain. The algorithms discussed in Section 3.1 allow us to assign membership probabilities to these objects, which is the best statistical way to deal with our limited knowledge. Nevertheless, each star that we observed either is or is not a member, and with a small sample, the assumption that a particular star has a membership probability of, e.g., 0.6 can produce different results than if it were known absolutely to be a member or not. Most of the stars in this category do not have an appreciable effect on the derived properties of Segue 1 (most importantly the velocity dispersion), either because they lie near the middle of the distribution or because their velocity uncertainties are relatively large. One object, however, can make a significant difference, as discussed in the following paragraph. A few other stars that cannot be classified very confidently in one category or the other are listed in the Appendix, but their inclusion or exclusion has minimal impact on the properties of Segue 1 or the results of this paper.

The one star that can individually affect the kinematics of Segue 1 is SDSSJ100704.35+160459.4. This star is a major outlier in velocity, with a mean velocity from two measurements of 231.6 ± 3.0 km s^{-1}. It is therefore located more than 6σ (where σ is estimated from the rest of the stars) away from the systemic velocity of Segue 1, but because its position is extremely close (38″) to the center of the galaxy and it has a CaT EW that could plausibly be associated with Segue 1 (although on the high side), the EM method returns a membership probability of 1. The membership probability from our full Bayesian analysis (see Paper II) is lower, but far from negligible, at 0.49. The high velocity of this star relative to the systemic velocity of Segue 1 could be explained if it is a member of a binary system, but our two velocity measurements of it (separated by 1 yr) do not show a significant change in velocity, so the period would have to be $\gtrsim$5 yr. In addition to its disproportionate effect on the velocity dispersion, for an equilibrium model a star that is a 6σ outlier from the mean velocity but is located so close to the center of the galaxy implies strongly radial orbits. None of the other stars in the sample lead to a preference for extreme velocity anisotropy.

5. THE INTRINSIC VELOCITY DISPERSION AND MASS OF SEGUE 1

Having carefully considered the membership of each star and the effects of the key outliers in the previous two sections, we are now in position to determine the best estimate of the intrinsic velocity dispersion of Segue 1 based on all available data. The full calculations that we use for this purpose are presented in Martinez et al. (2010), but we include a summary here for convenience.

5.1. Binary Correction Method

Given a sample of stars that may be members of Segue 1, we allow for the possibility that some of the observed stars are likely members of binary star systems rather than single stars. We therefore must treat the (unknown) velocity of the star system's

center of mass $v_{\rm cm}$ and the measured velocities themselves as distinct quantities. For each star system of absolute magnitude M_V, we have a set of measured velocities v_i, where i runs over the number of repeat observations of the star under consideration at times t_i, and the associated measurement uncertainties e_i. We write the likelihood of obtaining the observed data for each star assuming it is a member of Segue 1 (S1) in terms of a joint probability distribution in the measured velocities v_i and the unknown center-of-mass velocity $v_{\rm cm}$:

$$\begin{aligned}\mathcal{L}_{\rm S1}(v_i|e_i, t_i, M_V; \sigma, \mu, B, \mathscr{P}) &= \int_{-\infty}^{\infty} P(v_i|v_{\rm cm}, e_i, t_i, M_V; B, \mathscr{P}) P(v_{\rm cm}|\sigma, \mu) dv_{\rm cm} \\ &\propto (1-B)\frac{e^{-\frac{(\langle v\rangle-\mu)^2}{2\sigma^2}}}{\sqrt{\sigma^2+\sigma_m^2}} + BJ(\sigma, \mu|\mathscr{P}), \end{aligned} \quad (1)$$

where the first factor in the integrand is the probability of drawing a set of velocities v_i given a center-of-mass velocity $v_{\rm cm}$ and certain values for the binary parameters B and $\mathscr{P}$. B represents the binary fraction and $\mathscr{P}$ is the set of binary parameters $[\mu_{\log P}, \sigma_{\log P}]$ (see below). The second factor is the probability distribution of center-of-mass velocities given an intrinsic velocity dispersion of Segue 1, σ, and a systemic velocity, μ. In the last line of Equation (1), $\langle v\rangle$ is the average velocity weighted by measurement errors and σ_m is the uncertainty on this weighted average for the combined measurements of each star. Note that we assume that the center-of-mass velocity distribution of Segue 1 is Gaussian. We also use metallicity (W') and position to help determine membership, so that the full likelihood is of the form $\mathcal{L}(v_i, W', r)$, but we omit the metallicity and position dependence in the equations presented here for simplicity. The absolute magnitude of each star is taken into account so that its radius can be calculated and only binaries with separations larger than the stellar radius are allowed, as described in Minor et al. (2010) and Paper II.

For each star, the $J(\mu, \sigma|\mathscr{P})$ factor is generated by running a Monte Carlo simulation over the distribution of binary properties, which include the orbital period, mass ratio, and orbital eccentricity. Unfortunately, the characteristics of binary populations in dwarf galaxies are completely unknown at present. The best empirical constraints on binary properties come from studies of the Milky Way, but there is no guarantee that the small-scale star-forming conditions in the Milky Way and those that prevailed in Segue 1 many Gyr ago are similar, especially since Segue 1 has a metallicity two orders of magnitude below that of the Galactic disk population. In principle, a lower metallicity could change the probability of forming binary systems (and higher order multiples) and the properties of those systems, but binaries with separations in the range that can affect our observations ($\lesssim$10 AU) are expected to form via disk fragmentation (e.g., Kratter et al. 2010) or interactions between protostellar cores (e.g., Bate 2009), neither of which should be very sensitive to metallicity (M. Krumholz 2010, private communication).

In the Monte Carlo simulations, we fix the distributions of the mass ratio and eccentricity to follow that observed in solar neighborhood binaries. However, since the period distributions of binary populations have been observed to differ dramatically from cluster to cluster (e.g., Brandner & Koehler 1998; Patience et al. 2002), we allow for a range of period distributions. Specifically, we assume that the distribution of periods has a log-normal form similar to that of Milky Way field binaries (Duquennoy & Mayor 1991; Raghavan et al. 2010). We take the mean log period $\mu_{\log P}$ and the width of the period distribution $\sigma_{\log P}$ as free model parameters. We further assume that the period distribution observed in Milky Way field binaries is the result of superposing narrower binary distributions from a variety of star-forming environments. Thus, our prior on the period distribution is that it is narrower than, but consistent with being drawn from, the Duquennoy & Mayor (1991) period distribution with $\mu_{\log P} = 2.23$ and $\sigma_{\log P} = 2.3$. To accomplish this, we choose a flat prior in $\sigma_{\log P}$ over the interval [0.5, 2.3] and a Gaussian prior in $\mu_{\log P}$ centered at $\mu_{\log P} = 2.23$, with a width chosen such that when a large number of period distributions are drawn from these priors, they combine to reproduce the Milky Way period distribution of field binaries. We can then write the likelihood of each star being a member of Segue 1 or the Milky Way as

$$\begin{aligned}\mathcal{L}(v_i|e_i, t_i, M_V; f, B, \sigma, \mu, \mathscr{P}) &= (1-f)\mathcal{L}_{\rm MW}(v_i|e_i) \\ &+ f\mathcal{L}_{S1}(v_i|e_i, t_i, M_V; B, \sigma, \mu, \mathscr{P}), \end{aligned} \quad (2)$$

where f is the fraction of the total sample that are Segue 1 members. The second term in Equation (2) is given by Equation (1), and the likelihood of membership in the Milky Way is

$$\mathcal{L}_{\rm MW}(v_i|e_i) \propto \int \frac{e^{-\frac{(v_{\rm cm}-\langle v\rangle)^2}{2\sigma_m^2}}}{\sqrt{2\pi\sigma_m^2}} P_{\rm MW}(v_{\rm cm}) dv_{\rm cm}. \quad (3)$$

The expected Milky Way velocity distribution is taken from a Besançon model (Robin et al. 2003) after the same photometric criteria used to select Segue 1 stars have been applied.

5.2. Binary Correction Results

By applying the above analysis to our full Segue 1 data set, we can correct for the likely presence of binaries in the sample and derive the intrinsic velocity dispersion of the galaxy. All observed stars (not only the likely members) that meet the photometric selection cut described in Section 2.2 are included in this calculation, with the weight for each star determined by its likelihood of membership in Segue 1. Our posterior probability distribution for the dispersion is maximized at $\sigma = 3.7$ km s^{-1}, $\sim$12% smaller than what we measure without a binary correction. The 1σ uncertainties on the dispersion are +1.4 km s^{-1} and -1.1 km s^{-1}. We find a 90% lower limit on the dispersion of 1.8 km s^{-1}, and the probability of the true velocity dispersion being less than 1 km s^{-1} is $\sim$4%. The differential and cumulative probability distributions for σ are displayed in Figure 6. If the gravitational potential of Segue 1 were provided only by its stars, the velocity dispersion would be $\lesssim$0.4 km s^{-1} (G09). *Our lower limit on the dispersion therefore allows us to conclude with high confidence that Segue 1 is dynamically dominated by dark matter unless it is currently far from dynamical equilibrium.* We discuss the implausibility of large deviations from equilibrium caused by tidal forces later in Section 7.2.

We further note that small intrinsic velocity dispersions ($\sigma \lesssim 2$ km s^{-1}) can only be obtained if the binary period distribution is skewed toward short periods. In particular, mean periods of less than $\sim$40 yr are required to produce such a small dispersion (Paper II); for comparison, the mean period in the solar neighborhood is 180 yr (Duquennoy & Mayor 1991). The posterior distribution we derive for the mean period in Segue 1 is in fact weighted toward quite short periods ($\sim$10 yr).

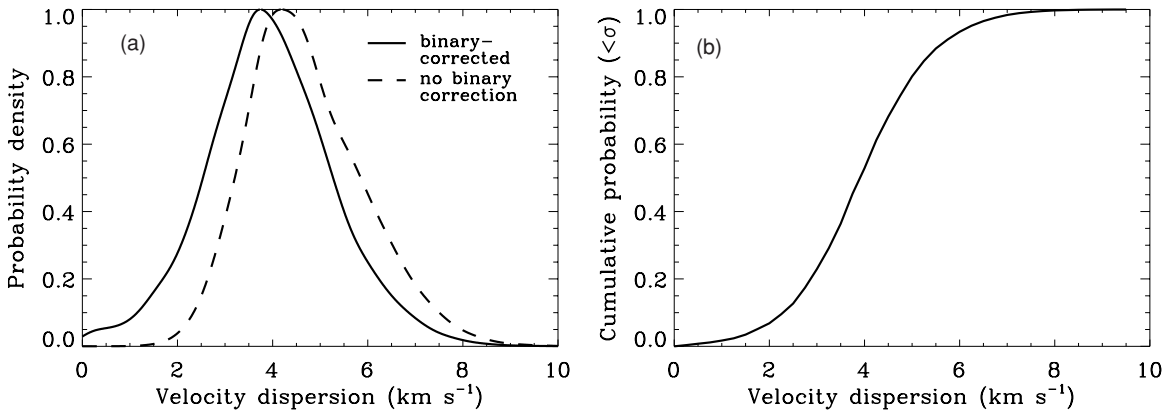

Figure 6. (a) Posterior probability distribution for Segue 1 velocity dispersion before (dashed) and after (solid) correcting for binary stars. (b) Cumulative probability distribution for Segue 1 velocity dispersion after correcting for binaries.

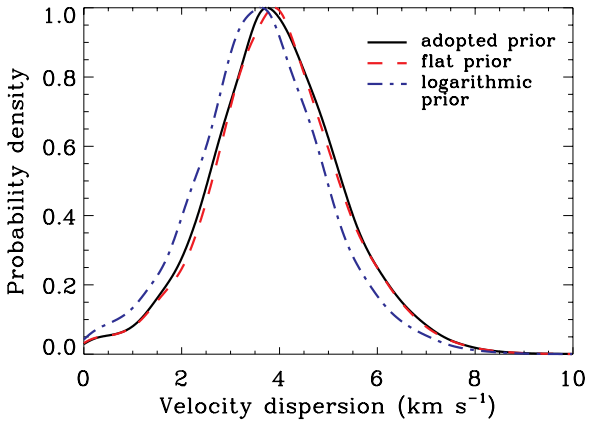

Figure 7. Effect of varying the prior distribution for the mean binary period on the derived velocity dispersion. The black solid curve shows on the Segue 1 velocity dispersion for our preferred assumption of the Milky Way field binary prior from Duquennoy & Mayor (1991). The dashed red curve represents a prior that is flat in $\mu_{\log P}$, and the dash-dotted blue curve illustrates the result of a logarithmic prior that is even more strongly biased toward short periods. The very small changes in both the most likely value of the velocity dispersion and the size of the tail to low values of the dispersion ($\sigma \leqslant 1$ km s^{-1}) demonstrate that our results are robust to differing assumptions about the binary population in Segue 1.

(A color version of this figure is available in the online journal.)

This result is not an artifact of the short time baseline of our multi-epoch data (observations on timescales of ∼1 yr cannot constrain periods of centuries or longer), because our priors allow for flatter period distributions than the posterior for the mean period. Despite this preference for shorter periods, the data strongly indicate only a modest contribution to the velocity dispersion from binaries because the period distribution is still wide and the small number of detected binaries indicates that the fraction of stars in close binary systems is not large.

To provide reassurance that our priors on the period distribution are not biasing the posterior period distribution toward longer periods (and hence the corrected velocity dispersion toward higher values), we repeated the calculations above with a flat prior on the mean period $\mu_{\log P}$. The best-fit mean period barely changed, and while somewhat shorter periods are allowed in this case, the probability of an intrinsic velocity dispersion less than 1 km s^{-1} does not increase (see Figure 7). Even with a more extreme logarithmic $\mu_{\log P}$ prior, the likelihood of a small dispersion is unchanged despite the resulting very short mean period. The reason for this outcome is that when the mean period is forced to be short, the binary fraction is then constrained to be low and the width of the period distribution is similarly constrained to be small to fit the observed changes in the velocities and the observed velocity distribution. Hence, the tail of the probability distribution toward low velocity dispersions cannot be made significantly larger by having a prior that biases the result to shorter mean periods.

These results contrast with the findings of McConnachie & Côté (2010), who conclude that galaxies like Segue 1 could have very low intrinsic velocity dispersions that are inflated substantially by the presence of binary stars. While we agree with their results given the assumptions they make, two primary factors are responsible for the different conclusions from our analysis. First, McConnachie & Côté ignore binaries with periods longer than 10–100 yr. This cutoff appears reasonable from an observational perspective, since such binaries will not be detectable in current data sets, but it has the effect of making the binary fractions they require very large because the majority of Milky Way binaries have periods longer than 100 yr. Second, they analyze only single-epoch velocity data sets, whereas the multiple measurements we have for a number of stars give us much greater leverage with which to determine the inflation of the velocity dispersion caused by binaries. Our Bayesian analysis including the multi-epoch data and all the information in the tail of the velocity distribution shows that a substantial inflation by binaries is disfavored for the Segue 1 data set presented here (see Paper II for more details).

5.3. Mass of Segue 1

The same Bayesian machinery described in Section 5.1 for determining the velocity dispersion of Segue 1 can also be employed to calculate the mass of the galaxy (again including a correction for binary stars). Wolf et al. (2010; also see Walker et al. 2009a) derived a simple formula for the mass within the half-light radius of a system: $M_{1/2} = 3\sigma^2 r_{1/2}/G$. For a flat prior on σ (see Paper II for a discussion of the effect of the choice of priors), we find a posterior probability distribution on the mass within the three-dimensional half-light radius of Segue 1 (38 pc) of $5.8^{+8.2}_{-3.1} \times 10^5\ M_\odot$, consistent with the mass determined by G09 from the original data set.[14] Because the uncertainties on

[14] Note that calculating $M_{1/2}$ directly from the stellar velocity data set with this Bayesian approach is not the same as simply plugging the derived values of σ and $r_{1/2}$ into the Wolf et al. (2010) formula. The final value for $M_{1/2}$ is very similar, but the uncertainties are more accurately determined (in particular the 2σ and 3σ confidence intervals) when we have determined the full probability distribution.

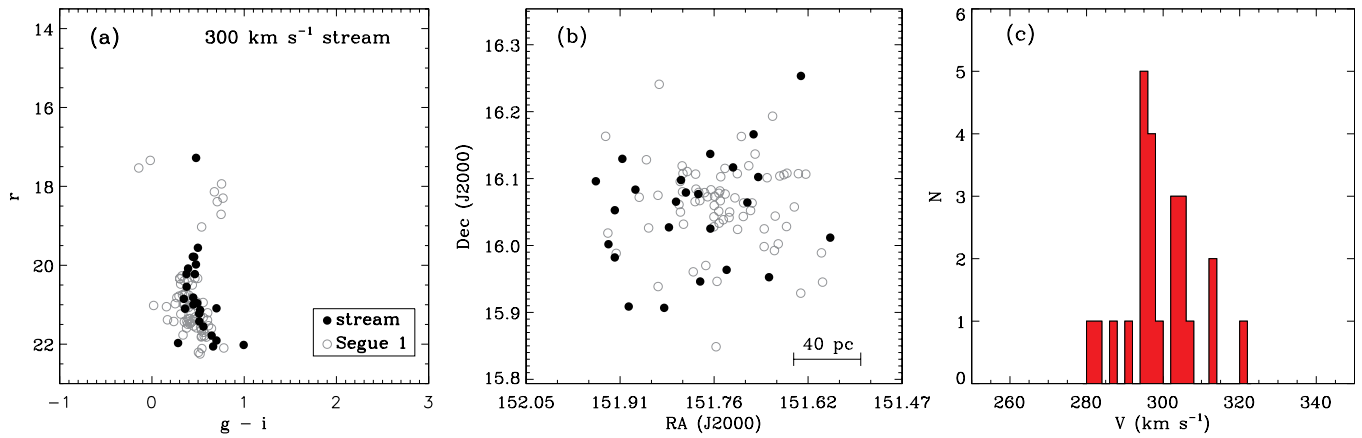

Figure 8. (a) Color–magnitude diagram of observed stars in the 300 km s^{-1} stream. The filled black circles represent the stars identified as candidate stream members, while the open gray circles are the Segue 1 members. (b) Spatial distribution of observed stars in the stream. Symbols are the same as in (a). (c) Velocity histogram of observed stars in the stream. Velocities are corrected to the heliocentric rest frame, and the velocity bins are 2 km s^{-1} wide.

(A color version of this figure is available in the online journal.)

the mass are not Gaussian, this measurement disagrees with the stellar mass of Segue 1 ($\sim$1000 $M_\odot$) at much more than 1.8σ significance; the 99% confidence lower limit on the mass is 16,000 $M_\odot$ (however, the magnitude of this low-mass/low-σ tail in the probability distribution is prior-dominated). The V-band mass-to-light ratio within the half-light radius is $\sim$3400 $M_\odot/L_\odot$. Since there is no evidence that the dark matter halo of Segue 1 is truncated at such a small radius, this value represents a lower limit on the total mass-to-light ratio of the galaxy, which could be 1–2 orders of magnitude larger.

6. A STREAM AT 300 km s^{-1}

In addition to Segue 1 and the Milky Way foreground, we clearly detect a third population of stars in our kinematic data, at a heliocentric velocity of 300 km s^{-1}. We refer to this structure as the "300 km s^{-1} stream" because of its lack of spatial concentration within our survey area. However, we recognize that these stars could still be part of a bound system as long as the angular size of the object is comparable to or larger than our field of view (diameter $\gg$20′, which corresponds to a physical size of at least 116 (d/20 kpc) pc). As an example, a galaxy similar to And XIX, which has a half-light radius of $\sim$1.7 kpc, would subtend several degrees at this distance (McConnachie et al. 2008).

G09 also recognized the existence of this stream, finding four stars in it among their smaller sample. We now present conclusive confirmation that this structure is real, with $\sim$20 stars in our new data set (see Figures 3–5). Because of the smaller member sample and the low contamination from Milky Way stars at such extreme velocities, the probabilistic membership algorithms described in Section 3.1 are not necessary in this case. Instead, we select stars that have velocities between 275 km s^{-1} and 325 km s^{-1} (the exact velocity limits are not important; see Figure 8(c)) and meet the same photometric criteria that were used for Segue 1. The color/magnitude screen eliminates five stars, leaving 24 likely members in the stream.

The color–magnitude diagram (CMD) of these stars is similar to that of Segue 1, indicating that the stream is also $\sim$20 kpc away (see Figure 8). The stream main sequence appears to be slightly redder (suggesting a higher metallicity) and slightly closer than Segue 1, although any differences are near the limit of what can be determined from the SDSS data. The stream stars are matched quite well with the fiducial sequence of the globular cluster M 5 ([Fe/H] = −1.27) from An et al. (2008), supporting the higher metallicity that one would have guessed by eye. By comparing to various globular cluster sequences, we estimate a distance of $\approx$22 kpc and a metallicity of [Fe/H] $\approx$ −1.3, but the uncertainties on both numbers are substantial.

The 24 candidate members have a mean velocity of 298.8 ± 1.7 km s^{-1} and a velocity dispersion of 7.0 ± 1.4 km s^{-1}, comparable to the dispersion of other known streams (Chapman et al. 2008; Grillmair et al. 2008; Odenkirchen et al. 2009; Newberg et al. 2010). Several of these stars may be foreground contaminants; in particular, the bright star at $g - i = 0.48$, $r = 17.60$ (SDSSJ100720.00+160137.5) is located a bit below the HB if the distance of 22 kpc preferred by the main-sequence fitting is used, although it does still lie within the AGB selection region shown in Figure 1. However, if the stream is at a slightly larger distance then this star could well be an HB member. The bluest of the faint stars (SDSSJ100650.83+160351.2; $g - i = 0.28$, $r = 21.97$) is $\sim$3σ away from the fiducial sequence used for the original target selection, and two other stars (SDSSJ100732.48+160500.5 and SDSSJ100708.38+155646.3) have reduced CaT EWs that are well above those of the bulk of the stream population. Even if we remove all four of these stars, the stream properties do not change significantly; the mean velocity in that case is 298.7 ± 1.5 km s^{-1} and the dispersion is 5.6 ± 1.2 km s^{-1}.

If we assume that the 300 km s^{-1} stream is a bound structure with a half-light radius larger than our survey area, the Wolf et al. (2010) formula implies a lower limit on the mass contained within its half-light radius of 5.3×10^6 (r/116 pc) $M_\odot$. This value would place the stream on the mass–radius relation of Milky Way dwarfs for a three-dimensional half-light radius of $\sim$500 pc (Wolf et al. 2010). On the other hand, it may be worth noting that the stream appears to be more extended in the east–west direction than north–south (cf. Figures 3(b) and 8(b)), consistent with an east–west extent. We therefore tentatively suggest that the 300 km s^{-1} stream could be the kinematic counterpart of the similarly oriented photometric feature identified by Niederste-Ostholt et al. (2009; see Section 7.1.1). An alternative possibility is that the stream might be related to Leo I, which is located approximately 3.°8 due south of Segue 1 at a similar velocity (282.9 ± 0.5 km s^{-1}; Mateo et al. 2008) and metallicity ([Fe/H] = −1.20; Kirby et al. 2011). Tracing the

stream with wider field spectroscopic data to test these hypotheses would be very desirable.

7. IS SEGUE 1 UNDERGOING TIDAL DISRUPTION?

Niederste-Ostholt et al. (2009, hereafter NO09) argued that rather than being a bound, dark matter-dominated dwarf galaxy, Segue 1 is a tiny star cluster whose apparent velocity dispersion has been inflated by contamination from the Sagittarius (Sgr) stream. We have demonstrated that Segue 1 is not a star cluster (Section 4.1), but that finding does not address the issues of tidal disruption or contamination. However, our new observations and a reanalysis of the SDSS data present some difficulties for the NO09 hypothesis. NO09 base their argument on several key points: (1) over a large area around Segue 1, there are very low surface density features whose CMDs are very similar to that of Segue 1 itself; (2) the surface brightness profile of Segue 1 appears to depart from a standard King or Plummer model at large radii; (3) the Fellhauer et al. (2006) model of the Sgr stream predicts that there should be some very old Sgr material near the position and velocity of Segue 1; (4) using SDSS blue horizontal branch (BHB) stars, a coherent feature that can probably be identified with the Sgr stream approaches the position and velocity of Segue 1; and (5) given the larger velocity dispersion of Sgr, only a small amount of contamination of the Segue 1 member sample by Sgr stars is necessary to substantially inflate the apparent velocity dispersion.

Below we discuss each of these ideas in turn and consider how our results affect their interpretation. We show that (1) while photometric tidal features are indeed present in this field, they appear more likely to be associated with other kinematically detected tidal structures rather than Segue 1; (2) in the radial range where the photometric and kinematic constraints are good, the surface brightness profile is well described by a Plummer model; (3) observational evidence for older wraps of the Sgr stream is non-existent, and even if present, more recent models suggest that this material has a very low surface density and differs in velocity from Segue 1; (4) the BHB feature identified by NO09 as potentially contaminating the Segue 1 data set is offset noticeably in both position and velocity from Segue 1; and (5) the resulting contamination has therefore been overestimated, and furthermore, these BHB stars seem to be associated with the Orphan Stream (in which case they are too spatially confined to affect observations near Segue 1) rather than the Sgr stream. We therefore conclude that contamination by Sgr stream stars does not have a significant impact on the measured velocity dispersion of Segue 1. We then consider the evidence that Segue 1 could be tidally disrupting, finding that while it is not possible to rule out recent tidal disturbances, the existing data do not provide significant support for such an interaction.

7.1. Reconsidering the Disrupting Cluster Scenario

7.1.1. Extended Tidal Debris Near Segue 1

As NO09 have shown, there is no doubt that there are spatially extended structures whose stars roughly follow the Segue 1 fiducial sequence distributed over a wide area around Segue 1. Within $\sim 1^\circ$ of Segue 1, this population is even visible by eye in SDSS CMDs.

What is less obvious is that these stars are necessarily associated with Segue 1. One alternative is that they are instead part of the Sgr stream. After all, it is clear from both observations (Belokurov et al. 2007a) and models (G09; Law et al. 2005) that the Sgr stream passes through this part of the sky at a distance similar to that of Segue 1. Indeed, at the position of Segue 1, the stream runs nearly east–west (Belokurov et al. 2006), exactly matching the orientation of the features identified by NO09. Another possibility is that the tidal features could be related to the 300 km s^{-1} stream, which also shares a very similar stellar population to Segue 1 (note that at the relevant distances, most of the stars detected by Sloan are on the main sequence, and thus the CMD filtering is primarily sensitive only to distance, not to metallicity). In either case, it seems more natural to associate this apparent tidal debris with one of the two known tidal structures at this position, rather than with the one object that is not obviously undergoing tidal disruption.

7.1.2. The Surface Brightness Profile of Segue 1

A second facet of the NO09 picture is the apparent excess of stars above the fitted Plummer, King, and exponential models at large radii. However, NO09 themselves note that the area covered by their deeper imaging is not large enough to define a meaningful background level, calling into question the significance of this excess. Within the radius probed by our kinematic data ($\sim$3 half-light radii), their photometric analysis shows that the data are fit well by a Plummer model, in agreement with the distribution of spectroscopically confirmed member stars that we derive (see Section 7.2). "Extratidal" excesses similar to the one claimed in the outer parts of Segue 1 have been seen in many other dwarf spheroidals (Irwin & Hatzidimitriou 1995; Majewski et al. 2000a, 2005; Martínez-Delgado et al. 2001; Palma et al. 2003; Walcher et al. 2003; Wilkinson et al. 2004; Mashchenko et al. 2005; Westfall et al. 2006; Muñoz et al. 2006; Sohn et al. 2007; Komiyama et al. 2007; Smolčić et al. 2007), but there is still no consensus regarding their physical significance (Peñarrubia et al. 2008, 2009).

7.1.3. Ancient Wraps of the Sagittarius Stream

The Sagittarius dwarf has both leading and trailing tidal streams stretching across the entire sky. The most recent wrap of the streams has been detected robustly in numerous ways (e.g., Ibata et al. 2001; Vivas et al. 2001; Dohm-Palmer et al. 2001; Bellazzini et al. 2003; Newberg et al. 2003; Majewski et al. 2003; Belokurov et al. 2006). Models predict that Sgr debris stripped on previous orbits may be present as well, but there is currently little observational evidence for such material. G09 showed that while Segue 1 is spatially coincident with the leading arm of the Sgr stream, the velocities of the recently stripped stars differ from that of Segue 1 by $\sim$100 km s^{-1}, firmly ruling out an association. NO09 pointed out that the Fellhauer et al. (2006) model predicts that there are also Sgr stars stripped several orbits earlier at this position that have velocities similar to Segue 1. In the most recent model by Law & Majewski (2010), which is the most successful to date in matching observations,[15] however, stars in this ancient wrap uniformly have much lower velocities in this part of the sky ($v_{\rm GSR} < 6$ km s^{-1}, compared with $v_{\rm GSR} = 113$ km s^{-1} for Segue 1). In addition, the surface density associated with the stars stripped at the earliest times should be overwhelmingly smaller than that of the more recent debris. Within 10° of Segue 1, the Law & Majewski (2010)

[15] While the Law & Majewski (2010) model provides a generally reasonable match to Sgr stream data, the bifurcation of the stream in the SDSS footprint is not yet fully understood and is not present in the model. Peñarrubia et al. (2010) argue that this structure can be a result of the original internal kinematics of the Sgr dwarf if its progenitor was a disk galaxy.

simulation contains $\gtrsim$200 times as many stars in the recently stripped, leading (negative velocity) stream as are present in the older, trailing stream. Since NO09 find similar numbers of stars in their observed positive and negative velocity BHB streams, this provides a strong argument that the BHB structure closer in velocity to Segue 1 is not, in fact, related to Sgr, as we discuss further in Section 7.1.5. Without any quantitative evidence for significant numbers of Sgr stream stars that are close in both position and velocity to Segue 1, we do not see any reason to expect substantial Sgr contamination of our Segue 1 member sample.

7.1.4. Does the Sagittarius Stream Overlap in Velocity With Segue 1?

NO09 also used SDSS observations of BHB stars to trace the kinematics of the *observed* Sgr debris near Segue 1 (while plenty of observations of Sgr stream velocities exist in other parts of the sky, the velocities near Segue 1 had not previously been measured). They found that the main component of the stream has negative heliocentric (and galactocentric) velocities at this position, more than 200 km s^{-1} away from the velocity of Segue 1, as pointed out by G09. Another coherent BHB component, though, is present at much higher velocities, similar to the prediction from Fellhauer et al. (2006) for older Sgr debris. NO09 concluded from this result that there is likely confusion between Segue 1 stars and Sgr stream stars in both position and velocity. However, *even accepting for the moment that these stars are actually part of the Sgr stream* (see Sections 7.1.3 and 7.1.5 for our counterarguments), two factors significantly diminish this confusion. First, the BHB stream identified by NO09 does not actually appear to reach the location of Segue 1; it peaks at $\delta \approx +24^\circ$, $\sim 8^\circ$ north of Segue 1, and seems to have petered out by the time it reaches Segue 1. Equally important is that the velocity of the BHB stars is $V_{\rm hel} \approx 195$ km s^{-1} ($V_{\rm GSR} \approx 132$ km s^{-1}), offset from the velocity of Segue 1 by 13 km s^{-1} in the heliocentric frame and 19 km s^{-1} in the galactic standard of rest (GSR) system.

7.1.5. Contamination of the Segue 1 Member Sample

Relying on the line of reasoning examined above, NO09 proposed that Segue 1 is actually a star cluster whose derived properties have been distorted by contamination from Sgr stream stars. Such contamination is a difficult issue to quantify, because by definition any stars that could be contaminating the member sample must have very similar velocities, metallicities, distances, and ages to Segue 1 stars. The only way to assess definitively the expected number of contaminants would be with an even wider field survey to identify Segue 1-like stars that are far enough away from the galaxy so as to be very unlikely to be associated. While SDSS includes some of the desired data, the SDSS spectroscopic coverage of stars at faint magnitudes is very sparse, so the vast majority of stars do not have velocity measurements. Nevertheless, some do, and those observations can be used to estimate the significance of the contamination.

The NO09 estimate of the contamination depends critically on the assumptions discussed in Section 7.1.4 that the BHB stream they identify with Sagittarius is exactly coincident in both position and velocity with Segue 1. However, as noted in Section 7.1.4, the surface density of BHB stars in the higher velocity component appears to be down by a factor of at least a few by the time it reaches Segue 1 (their Figure 10), and the velocity offset compared to Segue 1 further reduces the contribution of these stars within the Segue 1 velocity selection window.

To take into account these effects, we repeat the analysis described by NO09. Using DR7 data, if we select the BHB stars according to their heliocentric velocities, the positive velocity stream component has a mean velocity of $v_{\rm hel} = 195$ km s^{-1}. Since the stream is extended spatially, and therefore likely has a velocity gradient along its length, it is more concentrated in the GSR velocity system, where its velocity is $v_{\rm GSR} = 132$ km s^{-1} and its velocity dispersion is 12.2 km s^{-1} (corresponding to an intrinsic dispersion of 10 km s^{-1} after the 7 km s^{-1} median velocity errors are removed). Given the velocity window spanned by the likely Segue 1 members (not including SDSSJ100704.35+160459.4) of 194.6 km s^{-1} $\leqslant v_{\rm hel} \leqslant$ 224.2 km s^{-1}, only 41% of stars in the positive velocity stream would be expected to have velocities consistent with membership in Segue 1. Applying our actual photometric selection criteria (Section 2.2) instead of the broader selection box used by NO09 reduces our estimate of the surface density of Sgr stream stars at the declination of Segue 1 to 120 deg^{-2} (for stars with r magnitudes between 17.5 and 21.7). The complete region of our spectroscopic survey covers 0.087 deg^2, and the effective area of the full survey (including the incompleteness at larger radii) is $\sim$0.14 deg^2. Assuming, as NO09 did, that half of these stars are in the negative velocity stream component, and removing the 59% of the positive velocity stream stars that would still lie outside the Segue 1 velocity range, suggests that a total of 2–3 Sgr stream stars could be in our sample.

The next question is what effect including a few Sgr stars in an analysis of Segue 1 would have. We repeat the Monte Carlo simulation carried out by NO09 to answer this question. Using the same setup they did, with assumed velocity dispersions of 1 km s^{-1} for Segue 1 and 10 km s^{-1} for the Sgr stream (and putting them both at the same mean velocity, contrary to the argument above), we find that five Sgr stars must be included in the 71 star Segue 1 sample to have a significant chance ($\sim$20%) of boosting the apparent velocity dispersion of Segue 1 to at least 3.9 km s^{-1}. Given the smaller number of contaminating stars estimated above, we conclude that the inclusion of Sgr stream stars in the Segue 1 member sample is not likely to provide the dominant component of the observed velocity dispersion.

Also, when significant numbers of such contaminants are present they tend to have an easily visible effect on the velocity distribution (as they must if they are going to alter the dispersion). Visually, the simulated velocity histograms frequently appear to be composed of a narrow central peak containing most of the stars, surrounded by a few well-separated outliers (see Figure 9 for an example). These outliers would raise suspicions in any membership classification scheme like the ones outlined in Section 3.1 and might well be discarded from the sample. Interlopers that happen to fall within the main peak of the velocity distribution (and are therefore more difficult to identify) do not have a significant impact on the velocity dispersion; only stars in the wings of the distribution can both be mistaken for members and substantially change the apparent dispersion. However, our analysis shows that any such contaminating population cannot be large, and in Paper II we demonstrate that including an additional population does not change the derived parameters for Segue 1.

Moreover, a closer examination of the positive velocity stream component calls into question the assumption that it is associated with Sagittarius at all. Newberg et al. (2010) used BHB stars in SDSS and the SEGUE survey to trace the Orphan Stream across the sky and noted that it passes slightly north of Segue 1, at a distance of $\sim$25 kpc and a velocity of $v_{\rm GSR} = 130$ km s^{-1}.

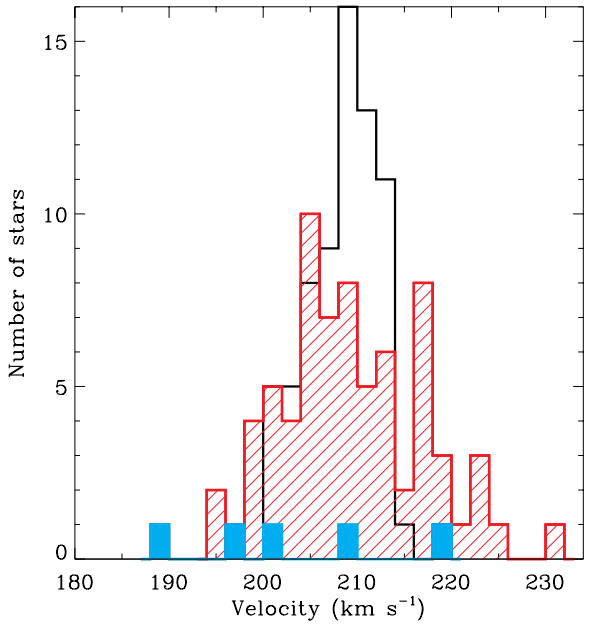

Figure 9. Monte Carlo simulation of the expected velocity distribution that would be obtained in the presence of significant contamination by the Sgr stream. We assume intrinsic dispersions of 1 km s^{-1} for Segue 1, 10 km s^{-1} for the Sgr stream, mean velocities of 208 km s^{-1} for both components, median velocity errors of 5 km s^{-1} (with a minimum of 2.2 km s^{-1}), and five Sgr stars in a 71 star sample. The velocities of the full simulated sample are shown by the black open histogram, with the Sgr contaminants overplotted as the filled cyan histogram and the observed Segue 1 stars as the red hatched histogram.

(A color version of this figure is available in the online journal.)

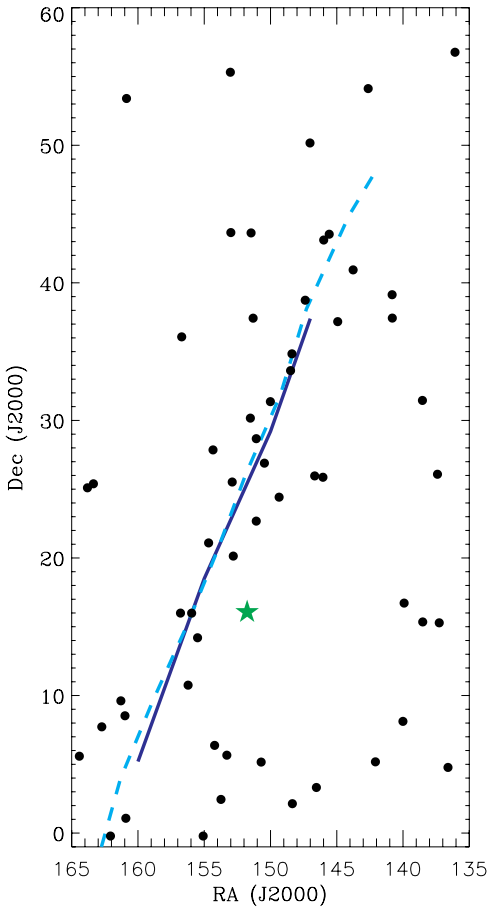

Figure 10. Spatial distribution of the BHB stars that can be confidently associated with the positive velocity stream identified by NO09. The green star marks the position of Segue 1, and the dashed cyan and solid blue lines indicate the traces of the Orphan Stream from Newberg et al. (2010) and Belokurov et al. (2007b), respectively. The close correspondence between the path of the Orphan Stream and the positions of the BHB stars at the same velocity suggests that these stars are members of the Orphan Stream rather than the Sagittarius stream.

(A color version of this figure is available in the online journal.)

Isolating the SDSS BHB stars within 1σ of the positive velocity stream's mean velocity, we find that their spatial distribution closely matches the track of the Orphan Stream determined by Belokurov et al. (2007b) and Newberg et al. (2010), as shown in Figure 10. The good correspondence between the path of the Orphan Stream and the BHB stars at the same velocity is highly suggestive that these stars are members of the Orphan Stream rather than an old (and heretofore undetected) wrap of the Sagittarius stream. If this peak is indeed related to the Orphan Stream, which is narrow and spatially confined, and not Sagittarius, then it is quite unlikely that any main-sequence stars associated with this feature would be located close enough to Segue 1 to appear as contaminants in our survey. That would then imply that most or all of the Sgr stars near Segue 1 are at negative velocities, as suggested in Section 7.1.3, which would further reduce our estimate of the possible contamination by Sgr above.

After considering each piece of evidence in concert, we thus conclude that contamination by the Sgr stream does not provide a very plausible explanation for the large velocity dispersion of Segue 1.

7.2. Signatures of Tidal Disruption

Having determined the nature of Segue 1, the effect of binary stars on the velocity dispersion, and the level of contamination by the Sgr stream, the final issue we must analyze is the impact of Milky Way tides. Unfortunately, while the presence of tidal tails would be incontrovertible evidence of tidal effects, the contrapositive is not true: there are no observations that can conclusively rule out tidal disruption. We therefore consider several possible signatures of tides.

1. First, our spectroscopic survey shows there are no obvious tidal tails connected to Segue 1 (see Figure 3). Although the spatial distribution is not uniform, we find Segue 1 members in every direction around the galaxy rather than the bipolar pattern that tidal tails would be expected to produce. The apparent clumpiness of the member stars toward the western edge of the galaxy may simply be the result of small number statistics (Martin et al. 2008). While the spectroscopic member sample confirms that Segue 1 has an elliptical shape, nonzero ellipticities are not necessarily associated with tidal influences (Muñoz et al. 2008) and may just reflect the shape with which the galaxy formed. We also note that the tidal tails seen in the SDSS photometry in the Segue 1 discovery paper (Belokurov et al. 2007a) have not been confirmed by deeper follow-up (Belokurov et al. 2007a; NO09; R. Muñoz et al. 2011, in preparation).
2. Velocity gradients are a commonly used indicator of tidal disruption, although like tidal tails they may only be visible in particular geometries and at large radii (Piatek & Pryor 1995; Muñoz et al. 2008; Łokas et al. 2008). We see no velocity gradient across Segue 1; the mean velocities of the stars in the eastern and western halves of the galaxy

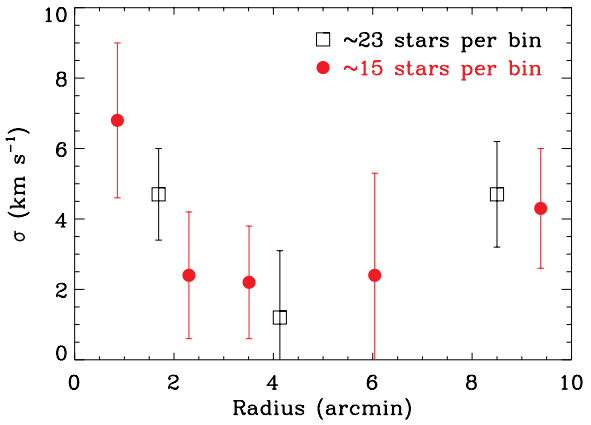

Figure 11. Velocity dispersion profile of Segue 1. The open squares show the profile obtained for bins of ∼23 stars each, and the filled red circles show the profile for bins of ∼15 stars. While the decrease in the velocity dispersion at intermediate radii (also visible in Figure 4) does not appear to be an artifact of the binning, it is only significant at the 1σ level.

(A color version of this figure is available in the online journal.)

agree within their uncertainties. The inclusion or exclusion of the ambiguous members, RR Lyraes, and binaries does not affect this result. There are also no apparent trends in the mean velocity from one end of the galaxy to the other (unlike, e.g., Willman 1; Willman et al. 2010). Using the methodology described by Strigari (2010) to calculate completely general constraints on the rotation of Segue 1, we derive a 90% confidence upper limit of 5.0 km s^{-1} on the rotation amplitude, but we note that samples a factor of two larger than ours are typically required to detect rotation.

3. A velocity dispersion profile that rises at large radii is often regarded as a possible result of tidal stripping, although the same behavior can be interpreted as evidence for an extended dark matter halo as well. Our member sample is not large enough to divide the data into more than a few radial bins, but we can begin to investigate the shape of the dispersion profile. Velocity dispersion profiles with two different binnings are displayed in Figure 11. As seen in the left panel of Figure 4, the velocity dispersion appears to reach a local minimum at a radius of ∼3′ before increasing back to its central value at larger radii. This shape seems to be independent of the exact binning chosen (and in fact is visible in the unbinned data), but as the error bars in the figure show, it is not statistically significant. While it is possible that the dispersion increase could suggest that the stars beyond ∼8′ from the center of the galaxy have been stripped, we caution that apparent features in other data sets of similar size (or even larger) have often disappeared when larger samples of velocity measurements become available (Wilkinson et al. 2004; Kleyna et al. 2004). With the modest number of bins possible for a sample of 71 members, we view the shape of the dispersion profile of Segue 1 as possibly interesting but not necessarily meaningful at this point. It is also worth pointing out that the mass implied by the central velocity dispersion, *even if the decline at ∼3′ is real*, is enough to put the tidal radius beyond the observed extent of the galaxy (see below), suggesting a consistency problem for the tidal interpretation.
4. Finally, "extratidal" excesses of stars at large radii are frequently considered to be indicative of tidal disturbances. The King (1962) tidal radius or limiting radius of Segue 1 is not well known because of the lack of deep enough wide-field photometry (although NO09 estimate a value of ∼26′), but our complete spectroscopic sample enables us to investigate the stellar profile out to $r \sim 13'$. Our observations are effectively complete within two half-light radii of the center of the galaxy (Section 2.6), where we identify 61 member stars. Between two and three times the half-light radius, we obtained successful spectra for 62 out of 75 stars located in the highest priority photometric selection region, for a completeness of 83%. We therefore adjust the nine observed members in that annulus to a projected total of 11 members, yielding 72 member stars within 3 half-light radii (13.′2). We find 39 member stars within $1r_{\rm half}$ (54% of the total), 22 member stars between $1r_{\rm half}$ and $2r_{\rm half}$ (31%), and estimate 11 member stars between $2r_{\rm half}$ and $3r_{\rm half}$ (15%), compared to the expected numbers of 56%, 33%, and 11% for a Plummer profile (once the 10% of the stars that should lie beyond $3r_{\rm half}$ are removed from consideration). The radial profile of Segue 1 thus does not show any excess out to at least $3r_{\rm half}$ (88 pc).

The above arguments demonstrate an absence of evidence in favor of tidal disruption, but as mentioned at the beginning of this section and discussed in detail by Muñoz et al. (2008), none of them (singly or in concert) are sufficient to prove that Segue 1 is not being tidally disrupted. Perhaps the strongest evidence for the absence of tidal effects results from consistency checks between the mass we measure for Segue 1, the corresponding tidal radius, and the timescale for tidal disruption.

As discussed by G09, the current position of Segue 1 is difficult to reconcile with a scenario in which it is in the final stages of disruption. Segue 1 has a crossing time of $\sim 10^7$ yr, and at a velocity of ∼200 km s^{-1} it will travel less than 2 kpc per crossing time. In order for the observed kinematics of Segue 1 to be significantly distorted by tides, the galaxy must be within a few crossing times of its orbital pericenter. Conservatively, then, Segue 1 should be no more than ∼10 kpc past pericenter. Segue 1 is located 28 kpc from the Galactic center, which would place its pericenter at a Galactocentric distance of at least 18 kpc, inconsistent with the closest approach to the Milky Way that would be required to disrupt it (see below).

For the IAU value of the Milky Way rotation velocity (220 km s^{-1}), the mass enclosed at the position of Segue 1 is $3 \times 10^{11}\ M_\odot$. The mass of Segue 1 is best constrained at the half-light radius of the galaxy (Wolf et al. 2010), where we obtain $M_{\rm half} = 5.8^{+8.2}_{-3.1} \times 10^5\ M_\odot$. Even if we assume (without any physical basis) that the mass distribution is arbitrarily truncated at the half-light radius, the instantaneous Jacobi radius (e.g., Binney & Tremaine 2008, Equation (8.91)) for Segue 1 would be ∼250 pc. If we use the Jacobi radius as an estimate of the tidal radius, then all of the stars we observed are well within the present-day tidal radius. Although Binney & Tremaine present a detailed discussion of why the Jacobi radius is necessarily an imperfect estimator, it is worth noting that subhalos in the Aquarius simulation (Springel et al. 2008) show a strong correlation between the radius of the subhalo and the Jacobi radius, supporting the use of the Jacobi radius as the tidal radius in practice. In order to bring the tidal radius in to the position of our outermost confirmed member, the pericenter of Segue 1's orbit must be less than ∼10 kpc. Substantially, disturbing stars *at the half-light radius*, where the mass is being measured, requires an orbital pericenter of less than ∼4 kpc (eccentricity greater than 0.75, since Segue 1 is clearly not near its apocenter at the present time). The Jacobi radius scales as $M_{\rm Segue\ 1}^{1/3}$, so even

major revisions to the derived mass do not affect our conclusion. This calculation is quite conservative, because it relies most strongly on the central kinematics of the galaxy where the observational uncertainties are smallest and tidal effects are weakest.

Incorporating reasonable assumptions about the extent of the dark matter halo of Segue 1 only strengthens this result. In the Via Lactea II simulation (Diemand et al. 2008), subhalos with $V_{\rm max} > 10$ km s^{-1} (see Section 8) that currently reside between 20 and 40 kpc from the host halo have median tidal truncation radii of ∼500 pc. Since these simulations self-consistently include tides and orbital trajectories, there is good reason to suspect that the mass of Segue 1 extends well past $r_{\rm half}$. If we extrapolate the Segue 1 mass beyond the observed region using cold dark matter (CDM) priors (since current simulations cannot resolve radii smaller than ∼100 pc), we find a mass within 100 pc of $M_{100} = 2.2 \times 10^6\, M_\odot$ and a mass within 300 pc of $M_{300} = 1.4 \times 10^7\, M_\odot$, consistent with the common mass scale of Milky Way satellites (Strigari et al. 2008a). With these larger masses, the current tidal radius would increase to 400–700 pc, making the center of Segue 1 nearly impervious to tides for any plausible orbit.

8. THE IMPORTANCE OF SEGUE 1 FOR DARK MATTER STUDIES

The large estimated mass of Segue 1 and its very small size (it has the smallest half-light radius of any known Local Group dwarf galaxy, with the possible exception of Willman 1) mean that Segue 1 also has the densest known concentration of dark matter. The average density enclosed within its half-light radius is $2.5^{+4.1}_{-1.9}\, M_\odot$ pc^{-3}, substantially higher than that found in other dwarf galaxies (Gilmore et al. 2007; Simon & Geha 2007; Walker et al. 2009a; Tollerud et al. 2011, Figure 17) or the solar neighborhood (e.g., Bahcall 1984). For comparison purposes, this density is equal to the ambient density of dark matter at $z \simeq 300$ and the average density of objects that collapsed at $z \simeq 50$. Given the extremely high mass-to-light ratio of Segue 1 (Section 5.3), it is safe to equate the dark matter density with the total density.

In the context of ΛCDM, densities as high as those that we infer within the half-light radius of Segue 1 are indicative of *massive* subhalos. Using the mass estimator from Wolf et al. (2010), the circular velocity at the half-light radius is related to the measured velocity dispersion via $V(r_{\rm half}) = \sqrt{3}\sigma \simeq 6.4$ km s^{-1}. This demands that $V_{\rm max} > 6.4$ km s^{-1} for the halo hosting Segue 1. Convolving the central circular velocity with CDM-based priors suggests that $V_{\rm max} > 10$ km s^{-1} (e.g., Bullock et al. 2010). Such halos are indeed found in the most advanced current *N*-body simulations (Diemand et al. 2008; Springel et al. 2008), demonstrating that the density of Segue 1 is reasonable in a ΛCDM universe, but how common it is for galaxies of Segue 1's luminosity to be found in very massive subhalos is not yet clear.

Since the flux of high-energy particles from dark matter annihilation scales as $\rho^2_{\rm DM} r^3/d^2$ and Segue 1 is also the second-nearest dwarf galaxy to the Sun, Segue 1 is clearly a high-priority target for indirect detection experiments (Martinez et al. 2009; Essig et al. 2009; Scott et al. 2010). Essig et al. (2010) use the sample of member stars presented here to carry out more detailed calculations of the expected gamma-ray and neutrino flux from dark matter annihilation in Segue 1. That analysis shows that Segue 1 is expected to be among the two brightest sources of annihilation radiation from Milky Way satellites and may be the brightest known dwarf galaxy. We strongly encourage future indirect detection searches for dark matter to target Segue 1.

Finally, the high density of Segue 1 provides important leverage for constraints on the phase-space density of dark matter particles, which is often estimated by the related quantity $Q_{\rm DM}(r) = \rho_{\rm DM}(r)/\sigma_{\rm DM}(r)^3$ defined by Hogan & Dalcanton (2000). Unfortunately, $Q_{\rm DM}$ cannot be measured directly from velocity dispersion data. While $\rho_{\rm DM}$ may be determined fairly accurately within $r_{\rm half}$, $\sigma_{\rm DM}$ is not observable. Generally, we expect $\sigma_{\rm DM} > \sigma_*$ (e.g., Wolf et al. 2010) because the dark matter velocity dispersion is governed by the total mass beyond the stellar radius (which cannot be measured). This implies that $\rho_{\rm DM}/\sigma^3_*$ provides only an *upper limit* on $Q_{\rm DM}$ at any particular radius. Some caution is advisable when reading the literature on this subject.

Given that $Q_{\rm DM}$ cannot be measured directly, we must rely on model fitting inspired by a theory prior in order to quantify $Q_{\rm DM}$ constraints from Segue 1. Of particular interest is the case of warm dark matter (WDM), where the primordial phase-space density may produce observationally accessible cores in the dark matter density. It is therefore useful to assume a dark matter density profile that is compatible with WDM rather than the usual CDM (Navarro et al. 1996 or similar) profile. We use a cored isothermal profile for illustration, which should have approximately the right shape for such models. With this profile and the kinematic data presented in this paper, we determine the posterior probability density for $Q_{\rm DM}$ at equally spaced logarithmic radii out to the stellar tidal radius following, e.g., Strigari et al. (2008b). We assume uniform priors on the scale radius and scale density for the isothermal profile, and we additionally make the assumption of velocity isotropy for the stars and the dark matter. Under these assumptions, we find a lower limit on the central value for $Q_{\rm DM}$ to be $\sim 10^{-3}\, M_\odot$ pc^{-3} (km s^{-1})$^{-3}$, higher than that determined for any other galaxy.[16] Estimates of this kind can place a lower limit on the allowed mass range for various WDM candidates, and we suggest that more detailed treatments of the phase-space density in Segue 1 to quantify these constraints would be very worthwhile.

9. SUMMARY AND CONCLUSIONS

We have presented a comprehensive spectroscopic survey of the ultra-faint Milky Way satellite Segue 1. The observations were designed both to search for potential tidal debris around Segue 1 and to constrain the effects of binary stars on its velocity dispersion. Within a radius of 10′ (67 pc) from the center of Segue 1, we measured the velocities of 98.2% of the candidate member stars. We identified 71 likely members, which we used to study the metallicity, kinematics, and nature of Segue 1.

The six red giants in Segue 1 have a mean metallicity of [Fe/H] = −2.5 and span a range of nearly 2 dex from [Fe/H] = −3.4 to [Fe/H] = −1.6. Both the presence of extremely metal-poor stars with [Fe/H] < −3 and the enormous metallicity spread demonstrate unambiguously that Segue 1 is a galaxy, rather than a globular cluster as some previous studies have suggested.

[16] SG07 list somewhat higher values for a few systems, but those were derived under much different assumptions (most notably, that mass follows light). For a consistent set of assumptions, Segue 1 has a higher phase-space density than any of the dwarfs analyzed there.

Using the new Bayesian method presented in our companion paper (Martinez et al. 2010), we analyzed the kinematics of the entire observed data set, allowing for contamination by Milky Way foreground stars and employing repeated velocity measurements for a subsample of the targets to correct for the effect of binary stars. We derived an intrinsic velocity dispersion of $3.7^{+1.4}_{-1.1}$ km s^{-1} for Segue 1 and only a 2% probability that the dispersion is small enough to be provided by the stellar mass of Segue 1 alone. The estimated mass contained within the half-light radius is $5.8^{+8.2}_{-3.1} \times 10^5\ M_\odot$, giving Segue 1 a V-band mass-to-light ratio at that radius of $\sim$3400 $M_\odot/L_\odot$.

Based on updated data and models, we re-examined earlier proposals that Segue 1 is tidally disrupting and that kinematic studies of it are likely to be contaminated by the Sagittarius stream. We showed that there is no observational evidence supporting the possibility of tidal disruption and that the tidal radius of Segue 1 has likely always exceeded its stellar extent unless it has an orbital pericenter around the Milky Way of less than $\sim$4 kpc. We also determined that contamination by Sgr stream stars is significantly lower than previously estimated; our current member sample is unlikely to contain more than three contaminants, which is not enough to substantially inflate the velocity dispersion.

Taken together, the results of our observations clearly point to the interpretation that Segue 1 is a dark matter-dominated galaxy—in fact, it has the highest mass-to-light ratio, and is therefore the darkest galaxy, yet found. The mean density inferred for Segue 1 within its half-light radius is consistent with the extrapolated density profiles of massive subhalos in high-resolution ΛCDM galactic halo simulations (Madau et al. 2008; Springel et al. 2008). The relative proximity of Segue 1 makes a strong case for considering Segue 1 in future searches for the products of dark matter annihilation processes (e.g., Essig et al. 2010). The density of dark matter within the inner 38 pc of Segue 1, $2.5^{+4.1}_{-1.9}\ M_\odot$ pc^{-3} or $\sim$100 GeV c^{-2} cm^{-3}, is the highest dark matter density yet determined, and consequently has broad implications for particle physics models and galaxy formation on small scales.

J.D.S. gratefully acknowledges the support of a Vera Rubin Fellowship provided by the Carnegie Institution of Washington. M.G. acknowledges support from NSF grant AST-0908752. Work at UCI was supported by NSF grant PHY-0855462 and NASA grant NNX09AD09G. Support for this work was also provided by NASA through Hubble Fellowship grant HST-HF-01233.01 awarded to E.N.K. by the Space Telescope Science Institute, which is operated by the Association of Universities for Research in Astronomy, Inc., for NASA, under contract NAS 5-26555. B.W. acknowledges support from NSF grant AST-0908193. This paper benefitted from the workshop "Shedding Light on the Nature of Dark Matter" held by the Keck Institute of Space Studies. We appreciate the contributions of the referee, who helped us clarify the paper. We thank Vasily Belokurov, Michael Cooper, Gerry Gilmore, Juna Kollmeier, Mark Krumholz, David Law, and George Preston for helpful conversations, and Matt Walker for providing his EM code. We also thank Alan McConnachie and Pat Côté for sharing a draft of their work on binary stars prior to publication. The analysis pipeline used to reduce the DEIMOS data was developed at UC Berkeley with support from NSF grant AST-0071048. This research has also made use of NASA's Astrophysics Data System Bibliographic Services.

Facilities: Keck:II (DEIMOS)

APPENDIX

COMMENTS ON THE MEMBERSHIP OR NON-MEMBERSHIP OF INDIVIDUAL STARS

In this appendix, we briefly discuss the case for membership or non-membership for several stars whose membership status is not clear-cut. Unlike SDSSJ100704.35+160459.4, however, the decision of whether to include or exclude these stars has no appreciable effect on the derived properties of Segue 1. We remind the reader that in the Bayesian approach used for our main results all of these stars (except the last two) are included in the calculations, weighted according to their membership probabilities. Other schemes generally require each star to be classified as either a member or non-member.

1. *SDSSJ100637.49+161155.1.* Very much like SDSSJ 100704.35+160459.4, SDSSJ100637.49+161155.1 sits perfectly on the Segue 1 fiducial sequence but has a significantly higher velocity (more than 3σ even for the largest possible value for the dispersion) than the galaxy. Given its relatively large distance from the center of Segue 1 (9.′7) and its higher than average CaT EW ($W' = 3.66$ Å), we consider this star unlikely to be a member. Its EM membership probability is 0.69 and its membership probability from Martinez et al. (2010) is 0.23.
2. *SDSSJ100622.85+155643.0.* SDSSJ100622.85+155643.0 has a very large uncertainty on its velocity measurement ($v = 223.9 \pm 37.8$ km s^{-1}) because of the low S/N of its spectrum and an apparently broad Hα line. Since much of the 1σ range for its velocity puts the star at a velocity consistent with Segue 1, we subjectively classified it as a member, but the statistical algorithms give it lower probabilities ($p = 0.73$ for EM and $p = 0.50$ for Martinez et al. 2010). However, the large velocity error means that SDSSJ100622.85+155643.0 receives essentially no weight in determining the Segue 1 velocity dispersion, so its true membership status is not important.
3. *SDSSJ100711.80+160630.4.* SDSSJ100711.80+160630.4 lies well outside the Segue 1 velocity range at $v = 247.1$ km s^{-1}, but also has a large velocity uncertainty of 15.9 km s^{-1}. The very high velocity led us to classify it as a non-member, but the objective techniques recognize that there is a reasonable chance that the star's actual velocity could be significantly lower, which might make it a member. Weighting its position near the center of Segue 1 quite heavily, the EM algorithm gives a membership probability of $p = 0.98$, while the Martinez et al. (2010) algorithm more conservatively estimates $p = 0.70$. Again, the large velocity error minimizes its impact on the derived velocity dispersion.
4. *SDSSJ100743.55+160947.2.* SDSSJ100743.55+160947.2 has a velocity near the high end of the Segue 1 velocity range ($v = 223.4 \pm 5.3$ km s^{-1}), but the uncertainty is large enough for it plausibly to be a member. In the CMD, it is located just outside the highest priority selection region, but again close enough that the photometric errors certainly allow it to be a member. We consider this star to be a probable member, but the objective algorithms give it moderate membership probabilities ($p = 0.87$ for EM and $p = 0.54$ for the Bayesian determination) because of its high velocity and large radius.
5. *SDSSJ100630.96+155543.6.* SDSSJ100630.96+155543.6 has a velocity several standard deviations smaller than the

systemic velocity of Segue 1, although the large velocity uncertainties (8.7 and 11.8 km s^{-1} for the two measurements) make this difference of marginal significance. Combined with its position 11.′6 from the center of the galaxy, the Martinez et al. (2010) algorithm hedges its bets at $p = 0.60$, while the EM membership probability is 0.94. This star is another probable member.

6. *SDSSJ100658.11+160701.4*. With a velocity of 187.0 ± 2.3 km s^{-1} and a $g - i$ color ∼0.25 mag blueward of the RGB (outside both the high- and low-priority CMD selection regions), SDSSJ100658.11+160701.4 appears to be a clear non-member star. However, the star could conceivably be an SX Phoenicis variable, in which case membership in Segue 1 would be possible, although as a variable star it would still be excluded from our analysis of the kinematics. SDSSJ100658.11+160701.4 is redder than would generally be expected for an SX Phoenicis star (e.g., Olech et al. 2005; Moretti et al. 2009), but we cannot rule out such a classification with the available data.
7. *SDSSJ100700.75+160300.5*. In our standard reduction of the data, using the arc spectrum obtained closest to the time of the observations, we were not able to determine a reliable velocity for SDSSJ100700.75+160300.5. The cross-correlation with the best-fitting template spectrum produced multiple widely separated cross-correlation peaks, with no obvious way to identify the correct solution. Switching to the arc frame from the end of the night (∼10 hr after the mask was observed) instead of the one from the afternoon (∼3 hr before the observations) produced a cleaner spectrum with a velocity of $v = 208.4 \pm 9.7$ km s^{-1}. Because none of the other spectra on this mask required such special treatment, and the increased time between calibrations and observations provides more opportunity for changes in the instrument, we regard this measurement as somewhat questionable and omit the star from our sample. It is probably a member of Segue 1, but with a velocity consistent with the systemic velocity of the galaxy and a large velocity error, including it would not change any of our results.

REFERENCES

Adelman-McCarthy, J. K., et al. 2007, ApJS, 172, 634
An, D., et al. 2008, ApJS, 179, 326
Anders, E., & Grevesse, N. 1989, Geochim. Cosmochim. Acta, 53, 197
Asplund, M., Grevesse, N., Sauval, A. J., & Scott, P. 2009, ARA&A, 47, 481
Bahcall, J. N. 1984, ApJ, 287, 926
Baltz, E. A., Briot, C., Salati, P., Taillet, R., & Silk, J. 2000, Phys. Rev. D, 61, 023514
Bate, M. R. 2009, MNRAS, 392, 590
Bellazzini, M., Ibata, R., Ferraro, F. R., & Testa, V. 2003, A&A, 405, 577
Belokurov, V., et al. 2006, ApJ, 642, L137
Belokurov, V., et al. 2007a, ApJ, 654, 897
Belokurov, V., et al. 2007b, ApJ, 658, 337
Belokurov, V., et al. 2009, MNRAS, 397, 1748
Belokurov, V., et al. 2010, ApJ, 712, L103
Binney, J., & Tremaine, S. 2008, Galactic Dynamics (2nd ed.; Princeton, NJ: Princeton Univ. Press)
Bovill, M. S., & Ricotti, M. 2009, ApJ, 693, 1859
Brandner, W., & Koehler, R. 1998, ApJ, 499, L79
Bringmann, T., Doro, M., & Fornasa, M. 2009, J. Cosmol. Astropart. Phys., JCAP01(2009)016
Bullock, J. S., Stewart, K. R., Kaplinghat, M., Tollerud, E. J., & Wolf, J. 2010, ApJ, 717, 1043
Carraro, G., & Lia, C. 2000, A&A, 357, 977
Carretta, E., Bragaglia, A., Gratton, R., & Lucatello, S. 2009, A&A, 505, 139
Carretta, E., et al. 2010, ApJ, 714, L7
Chapman, S. C., et al. 2008, MNRAS, 390, 1437
Clark, L. L., Sandquist, E. L., & Bolte, M. 2004, AJ, 128, 3019
Clem, J. L., Vanden Berg, D. A., & Stetson, P. B. 2008, AJ, 135, 682
Cohen, J. G., Kirby, E. N., Simon, J. D., & Geha, M. 2010, ApJ, 725, 288
Colafrancesco, S., Profumo, S., & Ullio, P. 2007, Phys. Rev. D, 75, 023513
Da Costa, G. S., Held, E. V., Saviane, I., & Gullieuszik, M. 2009, ApJ, 705, 1481
Dalcanton, J. J., & Hogan, C. J. 2001, ApJ, 561, 35
de Jong, J. T. A., Martin, N. F., Rix, H.-W., Smith, K. W., Jin, S., & Macciò, A. V. 2010, ApJ, 710, 1664
Diemand, J., Kuhlen, M., Madau, P., Zemp, M., Moore, B., Potter, D., & Stadel, J. 2008, Nature, 454, 735
Dohm-Palmer, R. C., et al. 2001, ApJ, 555, L37
Duquennoy, A., & Mayor, M. 1991, A&A, 248, 485
Essig, R., Sehgal, N., & Strigari, L. E. 2009, Phys. Rev. D, 80, 023506
Essig, R., Sehgal, N., Strigari, L. E., Geha, M., & Simon, J. D. 2010, Phys. Rev. D, 82, 123503
Evans, N. W., Ferrer, F., & Sarkar, S. 2004, Phys. Rev. D, 69, 123501
Faber, S. M., et al. 2003, Proc. SPIE, 4841, 1657
Fellhauer, M., et al. 2006, ApJ, 651, 167
Ferraro, F. R., et al. 2009, Nature, 462, 483
Fischer, P., Welch, D. L., Mateo, M., & Cote, P. 1993, AJ, 106, 1508
Geha, M., Willman, B., Simon, J. D., Strigari, L. E., Kirby, E. N., Law, D. R., & Strader, J. 2009, ApJ, 692, 1464 (G09)
Gilbert, K. M., et al. 2006, ApJ, 652, 1188
Gilmore, G., Wilkinson, M. I., Wyse, R. F. G., Kleyna, J. T., Koch, A., Evans, N. W., & Grebel, E. K. 2007, ApJ, 663, 948
Girardi, L., Grebel, E. K., Odenkirchen, M., & Chiosi, C. 2004, A&A, 422, 205
Grillmair, C. J., Carlin, J. L., & Majewski, S. R. 2008, ApJ, 689, L117
Hilker, M., Kayser, A., Richtler, T., & Willemsen, P. 2004, A&A, 422, L9
Hilker, M., & Richtler, T. 2000, A&A, 362, 895
Hogan, C. J., & Dalcanton, J. J. 2000, Phys. Rev. D, 62, 063511
Ibata, R., Irwin, M., Lewis, G. F., & Stolte, A. 2001, ApJ, 547, L133
Ideta, M., & Makino, J. 2004, ApJ, 616, L107
Irwin, M., & Hatzidimitriou, D. 1995, MNRAS, 277, 1354
Kaplinghat, M. 2005, Phys. Rev. D, 72, 063510
King, I. 1962, AJ, 67, 471
King, J. R., Stephens, A., Boesgaard, A. M., & Deliyannis, C. 1998, AJ, 115, 666
Kirby, E. N., Guhathakurta, P., Bolte, M., Sneden, C., & Geha, M. C. 2009, ApJ, 705, 328
Kirby, E. N., Guhathakurta, P., & Sneden, C. 2008a, ApJ, 682, 1217
Kirby, E. N., Lanfranchi, G. A., Simon, J. D., Cohen, J. G., & Guhathakurta, P. 2011, ApJ, 727, 78
Kirby, E. N., Simon, J. D., Geha, M., Guhathakurta, P., & Frebel, A. 2008b, ApJ, 685, L43
Kirby, E. N., et al. 2010, ApJS, 191, 352
Kleyna, J. T., Wilkinson, M. I., Evans, N. W., & Gilmore, G. 2004, MNRAS, 354, L66
Klimentowski, J., Łokas, E. L., Kazantzidis, S., Mayer, L., Mamon, G. A., & Prada, F. 2009, MNRAS, 400, 2162
Koch, A., et al. 2009, ApJ, 690, 453
Komiyama, Y., et al. 2007, AJ, 134, 835
Kraft, R. P., & Ivans, I. I. 2003, PASP, 115, 143
Kratter, K. M., Matzner, C. D., Krumholz, M. R., & Klein, R. I. 2010, ApJ, 708, 1585
Kuhlen, M., Diemand, J., & Madau, P. 2008, ApJ, 686, 262
Law, D. R., Johnston, K. V., & Majewski, S. R. 2005, ApJ, 619, 807
Law, D. R., & Majewski, S. R. 2010, ApJ, 714, 229
Lee, Y.-W., Joo, J.-M., Sohn, Y.-J., Rey, S.-C., Lee, H.-C., & Walker, A. R. 1999, Nature, 402, 55
Łokas, E. L., Klimentowski, J., Kazantzidis, S., & Mayer, L. 2008, MNRAS, 390, 625
Madau, P., Diemand, J., & Kuhlen, M. 2008, ApJ, 679, 1260
Majewski, S. R., Ostheimer, J. C., Patterson, R. J., Kunkel, W. E., Johnston, K. V., & Geisler, D. 2000a, AJ, 119, 760
Majewski, S. R., Patterson, R. J., Dinescu, D. I., Johnson, W. Y., Ostheimer, J. C., Kunkel, W. E., & Palma, C. 2000b, in Liege Int. Astrophys. Colloq. 35, The Galactic Halo: From Globular Cluster to Field Stars, ed. A. Noels et al. (Liege: Institut d'Astrophysique et de Geophysique), 619
Majewski, S. R., Skrutskie, M. F., Weinberg, M. D., & Ostheimer, J. C. 2003, ApJ, 599, 1082
Majewski, S. R., et al. 2005, AJ, 130, 2677
Marino, A. F., Milone, A. P., Piotto, G., Villanova, S., Bedin, L. R., Bellini, A., & Renzini, A. 2009, A&A, 505, 1099
Martínez-Delgado, D., Alonso-García, J., Aparicio, A., & Gómez-Flechoso, M. A. 2001, ApJ, 549, L63
Martinez, G. D., Bullock, J. S., Kaplinghat, M., Strigari, L. E., & Trotta, R. 2009, J. Cosmol. Astropart. Phys., JCAP06(2009)014

Martinez, G. D., Minor, Q. E., Bullock, J. S., Kaplinghat, M., Simon, J. D., & Geha, M. 2010, ApJ, submitted, arXiv:1008.4585 (Paper II)
Martin, N. F., de Jong, J. T. A., & Rix, H.-W. 2008, ApJ, 684, 1075
Martin, N. F., Ibata, R. A., Chapman, S. C., Irwin, M., & Lewis, G. F. 2007, MNRAS, 380, 281
Mashchenko, S., Couchman, H. M. P., & Sills, A. 2005, ApJ, 624, 726
Mateo, M., Olszewski, E. W., & Walker, M. G. 2008, ApJ, 675, 201
McConnachie, A. W., & Côté, P. 2010, ApJ, 722, L209
McConnachie, A. W., et al. 2008, ApJ, 688, 1009
McWilliam, A., & Smecker-Hane, T. A. 2005, ApJ, 622, L29
Minor, Q. E., Martinez, G., Bullock, J., Kaplinghat, M., & Trainor, R. 2010, ApJ, 721, 1142
Mizutani, A., Chiba, M., & Sakamoto, T. 2003, ApJ, 589, L89
Moretti, M. I., et al. 2009, ApJ, 699, L125
Muñoz, R. R., Geha, M., & Willman, B. 2010, AJ, 140, 138
Muñoz, R. R., Majewski, S. R., & Johnston, K. V. 2008, ApJ, 679, 346
Muñoz, R. R., et al. 2006, ApJ, 649, 201
Navarro, J. F., Frenk, C. S., & White, S. D. M. 1996, ApJ, 462, 563
Newberg, H. J., Willett, B. A., Yanny, B., & Xu, Y. 2010, ApJ, 711, 32
Newberg, H. J., et al. 2003, ApJ, 596, L191
Niederste-Ostholt, M., Belokurov, V., Evans, N. W., Gilmore, G., Wyse, R. F. G., & Norris, J. E. 2009, MNRAS, 398, 1771 (NO09)
Norris, J. E., & Da Costa, G. S. 1995, ApJ, 447, 680
Norris, J. E., Gilmore, G., Wyse, R. F. G., Yong, D., & Frebel, A. 2010a, ApJ, 722, L104
Norris, J. E., Wyse, R. F. G., Gilmore, G., Yong, D., Frebel, A., Wilkinson, M. I., Belokurov, V., & Zucker, D. B. 2010b, ApJ, 723, 1632
Odenkirchen, M., Grebel, E. K., Kayser, A., Rix, H.-W., & Dehnen, W. 2009, AJ, 137, 3378
Olech, A., Dziembowski, W. A., Pamyatnykh, A. A., Kaluzny, J., Pych, W., Schwarzenberg-Czerny, A., & Thompson, I. B. 2005, MNRAS, 363, 40
Olszewski, E. W., Pryor, C., & Armandroff, T. E. 1996, AJ, 111, 750
Palma, C., Majewski, S. R., Siegel, M. H., Patterson, R. J., Ostheimer, J. C., & Link, R. 2003, AJ, 125, 1352
Patience, J., Ghez, A. M., Reid, I. N., & Matthews, K. 2002, AJ, 123, 1570
Peñarrubia, J., Belokurov, V., Evans, N. W., Martínez-Delgado, D., Gilmore, G., Irwin, M., Niederste-Ostholt, M., & Zucker, D. B. 2010, MNRAS, 408, L26
Peñarrubia, J., Navarro, J. F., & McConnachie, A. W. 2008, ApJ, 673, 226
Peñarrubia, J., Navarro, J. F., McConnachie, A. W., & Martin, N. F. 2009, ApJ, 698, 222
Piatek, S., & Pryor, C. 1995, AJ, 109, 1071
Pieri, L., Pizzella, A., Corsini, E. M., Dalla Bontà, E., & Bertola, F. 2009, A&A, 496, 351
Preston, G. W., Sneden, C., Thompson, I. B., Shectman, S. A., & Burley, G. S. 2006, AJ, 132, 85
Queloz, D., Dubath, P., & Pasquini, L. 1995, A&A, 300, 31
Raghavan, D., et al. 2010, ApJS, 190, 1
Rey, S.-C., Lee, Y.-W., Ree, C. H., Joo, J.-M., Sohn, Y.-J., & Walker, A. R. 2004, AJ, 127, 958
Robin, A. C., Reylé, C., Derrière, S., & Picaud, S. 2003, A&A, 409, 523
Rubenstein, E. P., & Bailyn, C. D. 1997, ApJ, 474, 701
Rutledge, G. A., Hesser, J. E., & Stetson, P. B. 1997a, PASP, 109, 907
Rutledge, G. A., Hesser, J. E., Stetson, P. B., Mateo, M., Simard, L., Bolte, M., Friel, E. D., & Copin, Y. 1997b, PASP, 109, 883
Sand, D. J., Olszewski, E. W., Willman, B., Zaritsky, D., Seth, A., Harris, J., Piatek, S., & Saha, A. 2009, ApJ, 704, 898
Sand, D. J., Seth, A., Olszewski, E. W., Willman, B., Zaritsky, D., & Kallivayalil, N. 2010, ApJ, 718, 530
Scott, P., Conrad, J., Edsjö, J., Bergström, L., Farnier, C., & Akrami, Y. 2010, J. Cosmol. Astropart. Phys., JCAP01 (2010)031
Simon, J. D., & Geha, M. 2007, ApJ, 670, 313 (SG07)
Smolčić, V., Zucker, D. B., Bell, E. F., Coleman, M. G., Rix, H. W., Schinnerer, E., Ivezić, Ž., & Kniazev, A. 2007, AJ, 134, 1901
Sohn, S. T., et al. 2007, ApJ, 663, 960
Sollima, A., Beccari, G., Ferraro, F. R., Fusi Pecci, F., & Sarajedini, A. 2007, MNRAS, 380, 781
Springel, V., et al. 2008, MNRAS, 391, 1685
Strigari, L. E. 2010, Adv. Astron., 407394
Strigari, L. E., Bullock, J. S., Kaplinghat, M., Simon, J. D., Geha, M., Willman, B., & Walker, M. G. 2008a, Nature, 454, 1096
Strigari, L. E., Koushiappas, S. M., Bullock, J. S., Kaplinghat, M., Simon, J. D., Geha, M., & Willman, B. 2008b, ApJ, 678, 614
Tollerud, E. J., Bullock, J. S., Graves, G. J., & Wolf, J. 2011, ApJ, 726, 108
Tollerud, E. J., Bullock, J. S., Strigari, L. E., & Willman, B. 2008, ApJ, 688, 277
Toomre, A., & Toomre, J. 1972, ApJ, 178, 623
Tsuchiya, T., Dinescu, D. I., & Korchagin, V. I. 2003, ApJ, 589, L29
Vivas, A. K., et al. 2001, ApJ, 554, L33
Walcher, C. J., Fried, J. W., Burkert, A., & Klessen, R. S. 2003, A&A, 406, 847
Walker, M. G., Mateo, M., Olszewski, E. W., Bernstein, R., Wang, X., & Woodroofe, M. 2006a, AJ, 131, 2114
Walker, M. G., Mateo, M., Olszewski, E. W., Peñarrubia, J., Wyn Evans, N., & Gilmore, G. 2009a, ApJ, 704, 1274
Walker, M. G., Mateo, M., Olszewski, E. W., Sen, B., & Woodroofe, M. 2009b, AJ, 137, 3109
Walsh, S. M., Jerjen, H., & Willman, B. 2007, ApJ, 662, L83
Westfall, K. B., Majewski, S. R., Ostheimer, J. C., Frinchaboy, P. M., Kunkel, W. E., Patterson, R. J., & Link, R. 2006, AJ, 131, 375
Wilkinson, M. I., Kleyna, J. T., Evans, N. W., Gilmore, G. F., Irwin, M. J., & Grebel, E. K. 2004, ApJ, 611, L21
Willman, B., Geha, M., Strader, J., Strigari, L. E., Simon, J. D., Kirby, E., & Warres, A. 2010, AJ, submitted, arXiv:1007.3499
Willman, B., et al. 2005, AJ, 129, 2692
Wolf, J., Martinez, G. D., Bullock, J. S., Kaplinghat, M., Geha, M., Muñoz, R. R., Simon, J. D., & Avedo, F. F. 2010, MNRAS, 406, 1220
Yan, L., & Cohen, J. G. 1996, AJ, 112, 1489
Zucker, D. B., et al. 2006, ApJ, 643, L103